iScience

CellPress
OPEN ACCESS

Article

Rapamycin-sensitive mechanisms confine the growth of fission yeast below the temperatures detrimental to cell physiology

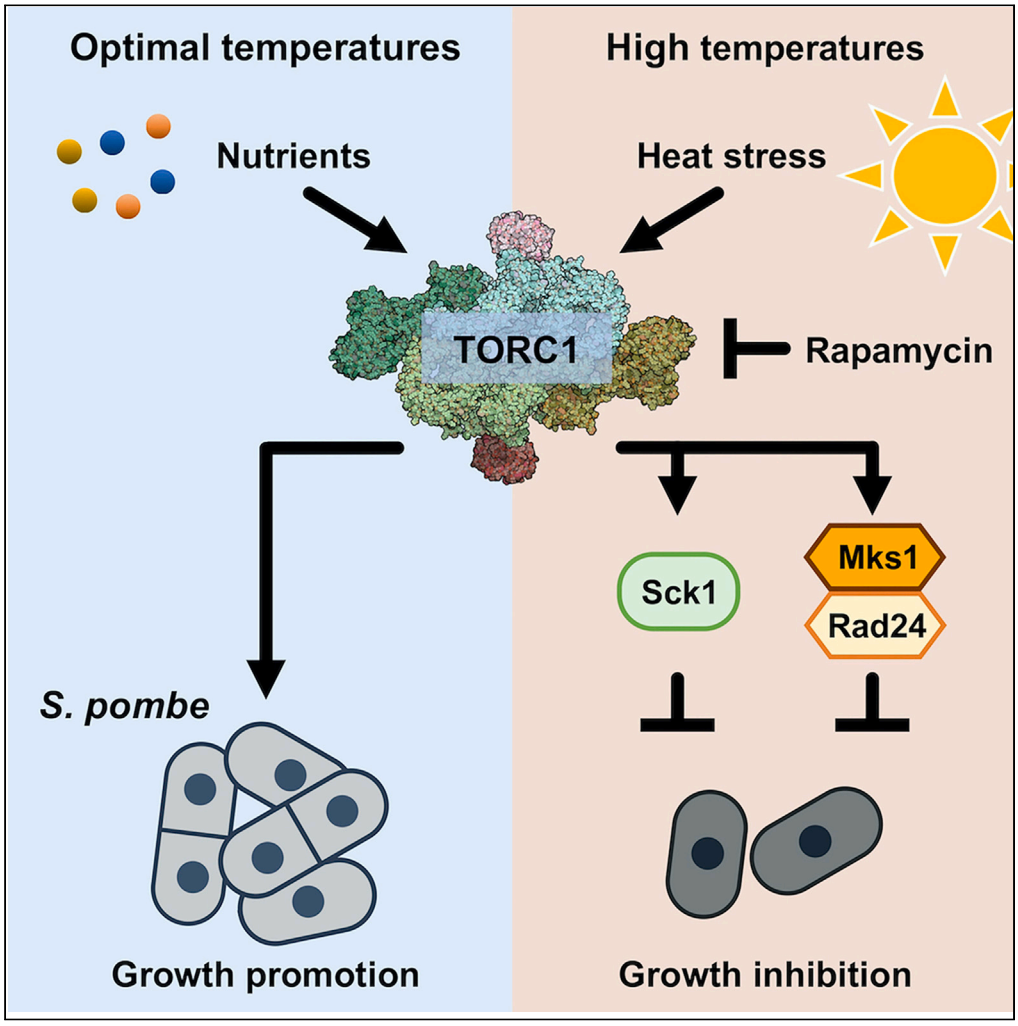

Yuichi Morozumi, Fontip Mahayot, Yukiko Nakase, ..., Ayu Shibatani, Kunihiro Ohta, Kazuhiro Shiozaki

y-morozumi@bs.naist.jp

Highlights

Suppression of TORC1 promotes the growth of *S. pombe* cells at high temperatures

Genome-wide screens identified several suppressors of high-temperature growth

Mks1 forms a complex with Rad24 to restrict cell growth at high temperatures

S. pombe has growth-restraint mechanisms below temperatures harmful to physiology

Morozumi et al., iScience 27, 108777
January 19, 2024
https://doi.org/10.1016/j.isci.2023.108777

iScience

CellPress
OPEN ACCESS

Article

Rapamycin-sensitive mechanisms confine the growth of fission yeast below the temperatures detrimental to cell physiology

Yuichi Morozumi,[1,5,6,*] Fontip Mahayot,[1,5] Yukiko Nakase,[1] Jia Xin Soong,[1] Sayaka Yamawaki,[1] Fajar Sofyantoro,[1,2] Yuki Imabata,[1] Arisa H. Oda,[3] Miki Tamura,[3] Shunsuke Kofuji,[1] Yutaka Akikusa,[1] Ayu Shibatani,[1] Kunihiro Ohta,[3] and Kazuhiro Shiozaki[1,4]

SUMMARY

Cells cease to proliferate above their growth-permissible temperatures, a ubiquitous phenomenon generally attributed to heat damage to cellular macromolecules. We here report that, in the presence of rapamycin, a potent inhibitor of Target of Rapamycin Complex 1 (TORC1), the fission yeast *Schizosaccharomyces pombe* can proliferate at high temperatures that usually arrest its growth. Consistently, mutations to the TORC1 subunit RAPTOR/Mip1 and the TORC1 substrate Sck1 significantly improve cellular heat resistance, suggesting that TORC1 restricts fission yeast growth at high temperatures. Aiming for a more comprehensive understanding of the negative regulation of high-temperature growth, we conducted genome-wide screens, which identified additional factors that suppress cell proliferation at high temperatures. Among them is Mks1, which is phosphorylated in a TORC1-dependent manner, forms a complex with the 14-3-3 protein Rad24, and suppresses the high-temperature growth independently of Sck1. Our study has uncovered unexpected mechanisms of growth restraint even below the temperatures deleterious to cell physiology.

INTRODUCTION

Although the habitat temperatures of living organisms are surprisingly diverse, each species has a relatively narrow range of optimal growth temperatures. Even a moderate rise in the growth temperatures can cause heat stress detrimental to the stability and/or activity of proteins.[1,2] As counteracting measures, cells activate the heat shock response, an evolutionarily conserved program that induces expression of the molecular chaperons termed heat shock proteins (HSPs).[3,4] The molecular chaperones maintain cellular proteostasis through refolding of denatured proteins, prevention of their aggregation, and sorting of unfolded proteins that are marked for degradation.[3,5] As the accumulation of misfolded protein aggregates is potentially harmful to cells,[2,6] molecular chaperones have been extensively studied as a major pro-survival mechanism in response to acute heat shock. On the other hand, it remains unclear whether proteotoxic stress is responsible for compromised or arrested growth of cells only marginally above their survivable temperatures.

The Target of Rapamycin (TOR), a member of the phosphoinositide-3 kinase-related kinase (PIKK) family, coordinates eukaryotic cell growth and proliferation with environmental cues, including nutrients and growth factors.[7] TOR functions by forming two distinct complexes, namely TOR complex 1 (TORC1) and TOR complex 2 (TORC2). The immunosuppressant rapamycin forms an intracellular complex with the FKBP12 protein, which then binds to the TOR kinase in TORC1 but not in TORC2, thereby leading to the specific inhibition of TORC1.[8,9] In response to nutrient and growth stimuli, TORC1 modulates anabolic processes, including the synthesis of proteins, nucleotides, and lipids, as well as cellular catabolism such as autophagy.[10,11]

Mammalian TORC1 (mTORC1), whose subunits include RAPTOR and mLST8, is regulated by two classes of small GTPases, RHEB and RAGs.[12,13] Upon amino acid stimuli, the active form of the RAG heterodimer (guanosine triphosphate [GTP]-bound RAGA/B with guanosine diphosphate [GDP]-bound RAGC/D) recruits mTORC1 to lysosomal membranes, where GTP-bound, active RHEB stimulates mTORC1 through direct interaction.[14,15] Activated mTORC1 then phosphorylates multiple substrates to promote cell growth. Ribosomal protein S6 kinase 1 (S6K1), an AGC-family kinase, and eukaryotic initiation factor 4E-binding protein 1 (4EBP1) are the best-characterized mTORC1 substrates that regulate mRNA translation.[16–19]

[1]Division of Biological Science, Nara Institute of Science and Technology, Ikoma, Nara 630-0192, Japan
[2]Faculty of Biology, Universitas Gadjah Mada, Sleman, Yogyakarta 55281, Indonesia
[3]Department of Life Sciences, Graduate School of Arts and Sciences, The University of Tokyo, Meguro-ku, Tokyo 153-8902, Japan
[4]Department of Microbiology and Molecular Genetics, University of California, Davis, Davis, CA 95616, USA
[5]These authors contributed equally
[6]Lead contact
*Correspondence: y-morozumi@bs.naist.jp
https://doi.org/10.1016/j.isci.2023.108777

The TORC1 signaling pathway is highly conserved between mammalian cells and the fission yeast *Schizosaccharomyces pombe*.[20] In *S. pombe*, the catalytic subunit Tor2 forms TORC1 together with the RAPTOR equivalent Mip1 and Wat1/Pop3, an mLST8 ortholog.[21–23] The fission yeast RHEB ortholog termed Rhb1 functions as an essential activator of TORC1,[24–26] while TORC1 is negatively regulated by the Gtr1-Gtr2 heterodimer, which is a counterpart of the mammalian RAGA/B-RAGC/D complex.[27,28] Psk1, an AGC-family kinase orthologous to mammalian S6K1, has been identified as a substrate of TORC1.[29,30] TORC1 is essential for cell growth, and the loss of the TORC1 function leads to cell-cycle arrest in G1 in both budding and fission yeasts.[8,21–23,26,31] On the other hand, suppression of TORC1 by rapamycin brings about no apparent growth inhibition in fission yeast,[32] in stark contrast to the observation in budding yeast[33]; rapamycin appears to only partially inhibit the TORC1 activity in *S. pombe*.[34]

Studies in the budding yeast *Saccharomyces cerevisiae* have implicated TORC1 in not only cellular growth control but also diverse physiological responses.[35,36] Budding yeast cells respond to mitochondrial dysfunction by activating the retrograde (RTG) signaling pathway, which regulates the expression of a set of genes involved in lysine biosynthesis and the tricarboxylic acid (TCA) cycle (RTG target genes). The Mks1 protein has been characterized as a negative regulator of the RTG pathway.[37–39] Mks1 is phosphorylated in a TORC1-dependent manner and binds to the 14-3-3 protein Bmh1.[37,40,41] The resulting complex inhibits the nuclear translocation of transcription factors involved in the expression of RTG target genes.[41] In fission yeast, open reading frame SPAC1420.01c encodes a protein with limited homology to budding yeast Mks1 with a conserved short stretch in the N-terminal region (Figure S1). This Mks1-like protein in fission yeast has not been characterized.

The optimal growth temperature of *S. pombe* cells is around 30°C; they exhibit somewhat impaired growth at 37°C and fail to grow at 38°C and above. We have found that fission yeast cells remain viable and proliferate even at 39°C when the TORC1 activity is suppressed by rapamycin. Moreover, the null mutant of the Sck1 kinase, a known TORC1 substrate,[29,42] exhibits significant cell growth at 39°C even in the absence of rapamycin. Thus, unexpectedly, the growth of fission yeast cells at high temperatures appears to be negatively regulated by TORC1, which has been established as a growth promoter in *S. pombe* and other eukaryotes. Furthermore, our genome-wide screens have identified several additional factors, including Mks1, that appear to restrict cellular growth at high temperatures. These findings strongly suggest that the high-temperature growth of fission yeast is impeded by inherent mechanisms even below the temperatures detrimental to cell physiology. Although the heat sensitivity of cell growth is a ubiquitous phenomenon, it may not necessarily be due to proteotoxic stress or other heat-induced damage to cellular components.

RESULTS

Suppression of TORC1 activity promotes *S. pombe* growth at high temperatures

In the fission yeast *S. pombe*, the optimal growth temperature of wild-type cells is around 30°C, and their growth is significantly impaired at 38°C and completely ceased at 39°C or higher (Figure 1A, left). We serendipitously discovered that fission yeast cells exhibit significant proliferation even at 38°C and 39°C, but not at 40°C, on agar medium supplemented with rapamycin, a TORC1-specific inhibitor (Figure 1A, right). Such enhanced growth at 39°C was also observed when culturing *S. pombe* cells in liquid medium with rapamycin, though their proliferation rate and the cell density in the plateau phase were not as high as those at 30°C (Figure 1B). The suppression of the TORC1 activity by rapamycin was confirmed by the loss of phosphorylation in Psk1, a TORC1 substrate in fission yeast (Figure S2A).[29] The cell viability assay with methylene blue staining[43,44] indicated that, at 39°C, cell viability was largely lost by 48 h, which was counteracted by rapamycin (Figure 1C).

When exposed to heat stress, fission yeast cells induce the expression of a set of HSPs, such as Hsp16, to maintain the cellular proteostasis.[45] Accumulation of the Hsp16 protein expressed with the GFP epitope from the *hsp16*$^{+}$ locus was observed after a temperature shift to 39°C, similarly in both the presence and absence of rapamycin (Figure S2B). Thus, the high-temperature growth of fission yeast in the presence of rapamycin does not appear to be due to the enhanced expression of the HSP.

In various model organisms, including fission yeast, heat resistance is improved by exposing cells to mild heat stress, allowing them to survive subsequent severe heat shock.[46,47] We therefore examined whether fission yeast pretreated with mild heat stress can proliferate at high temperatures. With pretreatment of cells at 37°C for 30 min, their viability during acute heat shock (48°C for 15 min) increased significantly, but they failed to grow at 39°C (Figure S2C). Similar acquired resistance to the acute heat shock was observed with stationary-phase cells (Figure S2D, upper panel), which exhibit enhanced resistance to diverse stress conditions.[48,49] However, those cells that experienced the stationary phase did not grow better at 39°C compared to cells from a log-phase culture (Figure S2D, lower panels). Thus, the acquired heat resistance of cells exposed to mild heat stress or in the stationary phase may be transient and does not promote continuous cell proliferation under high-temperature conditions.

To further corroborate the effect of rapamycin on high-temperature proliferation of fission yeast cells, the growth of a mutant strain lacking Fkh1, an FKBP12 ortholog that mediates rapamycin-dependent inhibition of TORC1,[50–52] was examined at high temperatures. As expected, the *fkh1* null mutant failed to grow at 39°C even in the presence of rapamycin (Figure 1D), consistent with the idea that the rapamycin-induced heat resistance is due to TORC1 inhibition. Furthermore, even in the absence of rapamycin, mutations to the TORC1 subunit Mip1, a RAPTOR ortholog,[21–23] allowed fission yeast cells to grow at high temperatures (Figure 1E). Strains carrying *mip1-R358A*, *mip1-R504A*, or *mip1-Y533A* mutations have attenuated TORC1 activity,[30] and they grew at 39°C whereas *mip1*$^{+}$ cells failed to do so.

Taken together, these results indicate that suppression of TORC1 activity allows *S. pombe* cells to remain viable and proliferate at growth-inhibitory high temperatures up to 39°C.

TORC1-Sck1 signaling suppresses cellular growth at high temperatures

The aforementioned results imply that TORC1 activity somehow restricts cell growth at high temperatures. To further explore the events downstream of TORC1 in the control of high-temperature growth, we examined the phenotypes of the null mutants that lack the known

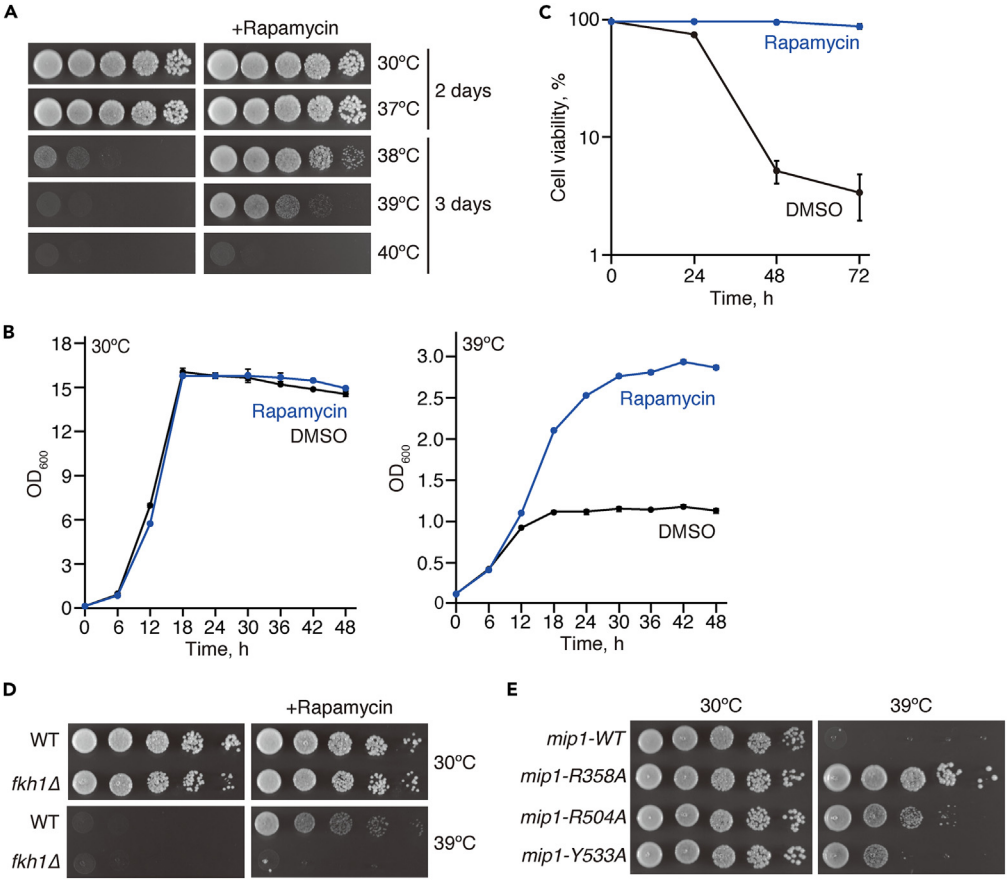

Figure 1. Suppression of TORC1 activity allows *S. pombe* cells to grow at high temperatures

(A) Wild-type cells were grown in YES liquid medium at 30°C. Their serial dilutions were spotted onto YES agar plates in the presence and absence of 100 ng/mL rapamycin for growth assay at 30°C and 37°C for 2 days, and at 38°C, 39°C, and 40°C for 3 days.

(B) Wild-type cells were grown in YES liquid medium at 30°C. At 0 h, the initial OD was adjusted to OD_{600} = 0.1 ± 0.02, and the cell growth in the presence and absence of 200 ng/mL rapamycin at 30°C and 39°C was monitored by measuring OD_{600} at indicated time points. Data are presented as means ± standard deviation (SD) from three independent experiments.

(C) Wild-type cells were grown in YES liquid medium at 30°C. At time 0, the culture concentration was adjusted to OD_{600} = 0.1 ± 0.05, and the cell viability in the presence and absence of 200 ng/mL rapamycin at 39°C was measured by methylene blue staining at indicated time points. Data are presented as means ± SD from three independent experiments, and at least 200 cells were counted for each experiment.

(D) The *fkh1Δ* mutant failed to grow at 39°C even in the presence of rapamycin. The growth of wild-type (WT) and *fkh1Δ* cells was tested as in (A).

(E) The *mip1* mutants exhibit cell proliferation at 39°C even in the absence of rapamycin. The indicated *mip1* mutant strains were grown in YES medium at 30°C, and their serial dilutions were spotted onto YES agar plates for growth assay at 30°C and 39°C. See also Figure S2.

TORC1 substrates in fission yeast; the AGC-family kinases Psk1, Sck1, and Sck2[29]; the RNA polymerase III repressor Maf1[53]; and the autophagy regulator Atg13.[42] Among them, only the *sck1* null mutant (*sck1Δ*) exhibited growth at 39°C even in the absence of rapamycin (Figure 2A). A similar heat-resistant phenotype was observed with a strain expressing the catalytically inactive Sck1 kinase, Sck1KD, in which Lys-331 in the ATP-binding domain is substituted with alanine (Figure 2B). These results suggest that TORC1-dependent activation of the Sck1 kinase negatively regulates cell growth at high temperatures.

We also assessed the phosphorylation state of Sck1 at high temperatures. The FLAG epitope-tagged Sck1 protein phosphorylated by TORC1 is detectable as a band with less electrophoretic mobility,[27,30] which disappeared in the presence of rapamycin at both 30°C and 39°C (Figure 2C). It was found that the total amount of Sck1 protein increased after the temperature shift from 30°C to 39°C, leading to the accumulation of its phosphorylated form as well.

A genome-wide screen for genes inhibitory to cellular growth at high temperatures

Our findings described earlier revealed that *S. pombe* has mechanisms to proactively suppress cell growth at high temperatures, such as 39°C, including TORC1-Sck1 signaling. For more comprehensive identification of the regulatory elements that restrict high-temperature growth, we screened a haploid null mutant library of approximately 3,400 nonessential genes for mutants that can grow at 39°C. Not surprisingly, the screen

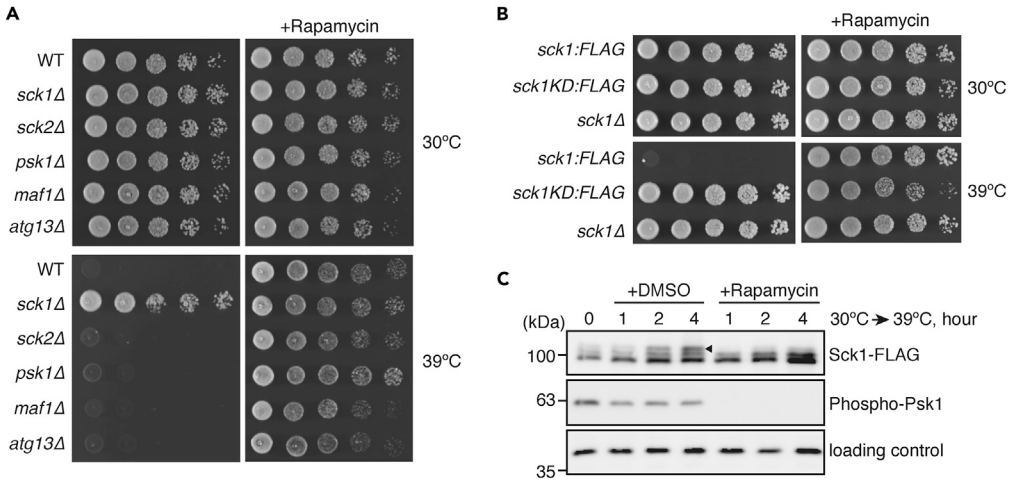

Figure 2. The Sck1 kinase inhibits cell growth at high temperatures

(A) Wild-type (WT) and the indicated null mutant cells were grown in YES liquid medium at 30°C. Their growth in the presence and absence of rapamycin (100 ng/mL) was tested at 30°C and 39°C by spotting the serial dilutions of their cultures on YES agar plates.

(B) The catalytic activity of Sck1 is required for suppressing high-temperature growth. The growth of the *sck1:FLAG*, *sck1-K311A: FLAG*, and *sck1Δ* strains was tested as in (A).

(C) TORC1-dependent phosphorylation of Sck1 at high temperatures. The *sck1:FLAG* strain was grown in YES medium at 30°C and shifted to 39°C in the presence and absence of 200 ng/mL rapamycin. Cells were harvested at indicated time points, and their cell lysate was subjected to immunoblotting using anti-FLAG, anti-phospho-S6K1 (Phospho-Psk1) and anti-Spc1 (loading control) antibodies. An arrowhead represents the Sck1 protein phosphorylated by TORC1.

re-isolated the *sck1Δ* mutant, along with the null mutants of SPAC1420.01c, *dri1*$^+$, SPBC17D1.05, and *mtq2*$^+$ (Figure 3A). Because the protein encoded by SPAC1420.01c has some homology to budding yeast Mks1 (Figure S1 and introduction), it is referred to as Mks1 hereafter. Dri1 is a putative RNA-binding protein involved in heterochromatin assembly and kinesin loading to the mitotic spindle,[54,55] while SPBC17D1.05 is an uncharacterized, fission yeast-specific protein, which we named Rhs1 (Regulator of heat sensitivity). The growth of the *S. pombe mks1*Δ mutant at 39°C was comparable to that of *sck1*Δ and better than that of the *dri1*Δ, whose growth phenotype was similar to that of *rhs1Δ* (Figure 3A). Among the isolated mutants, only *mtq2Δ* cells showed compromised growth even at 30°C and 34°C, though they also grew at 39°C (Figures 3A and S3A). Mtq2 is predicted to be the catalytic subunit of the eRF1 methyltransferase complex; its ortholog in *S. cerevisiae* forms a heterodimer with Trm112 to methylate the translation release factor eRF1, which is essential for translation termination.[56,57]

Like in wild-type cells treated with rapamycin, the induction of Hsp16 in response to the temperature shift from 30°C to 39°C was not significantly affected by the *sck1*Δ and *mks1*Δ mutations (Figure S3B); thus, the high-temperature growth of those mutants may not be attributed to the hyperactivation of the HSP system. It has been reported that adaptation of cells to high-temperature conditions can accompany a growth trade-off at low temperatures, resulting in a shift in the growth temperature range.[58,59] However, comparable growth was observed among the wild-type, *sck1*Δ, *mks1*Δ, *dri1*Δ, and *rhs1*Δ strains at 16°C and 14°C, where rapamycin also did not affect their growth (Figure S3C).

In order to examine the functional relationships among the genes identified in the screen, their double mutants were constructed for epistasis analyses. Growth kinetics monitored in liquid medium at 30°C found no apparent difference among the wild-type, *mks1Δ*, *sck1Δ*, and *sck1Δ mks1Δ* strains. At 39°C, all of those mutants exhibited significant cell proliferation in comparison to the wild-type strain, though not as robust as that at 30°C (Figure 3B). Notably, the deletion of the two genes showed an additive effect, and the *sck1Δ mks1Δ* double mutant grew better than the individual single mutants, suggesting that Mks1 and Sck1 function independently to negatively regulate cell proliferation at high temperatures. Similar additive effects were also observed when the *sck1Δ* or *mks1Δ* mutations were combined with either *dri1Δ* or *rhs1Δ* (Figure S4). On the other hand, the growth of the *dri1Δ rhs1Δ* double mutant at 39°C was comparable to that of the respective single mutants when cultured in liquid medium (Figure 3C) as well as on solid agar medium (Figure 3D). These observations suggest that Dri1 and Rhs1 function in the same pathway, but independently of Sck1 and Mks1. Interestingly, a fission yeast interactome study using the yeast two-hybrid assay detected the interaction between Dri1 and Rhs1.[60] To examine whether Dri1 forms a complex with Rhs1, we constructed a strain where the chromosomal *dri1*$^+$ gene is tagged with the *myc* epitope sequence, and the Rhs1 protein is expressed with the FLAG epitope from the *rhs1*$^+$ locus. Immunoprecipitation using anti-FLAG affinity beads revealed that FLAG-tagged Rhs1, which is detectable as a thick band due to its phosphorylation (Figure S3D), associates with Dri1 at both 30°C and 39°C (Figure 3E). It is therefore likely that Dri1 and Rhs1 function as a complex in the suppression of cell growth at high temperatures.

A mutation to the 14-3-3 protein Rad24, which forms a complex with Mks1, confers heat resistance on *S. pombe* cells

In addition to screening the gene deletion library as described earlier, we also attempted to isolate spontaneous mutations that confer heat resistance to fission yeast cells. When a wild-type strain was incubated at 39°C on agar growth medium, viable mutant colonies appeared at a frequency of ~1 × 10^{-5}, which were subsequently analyzed by whole-genome sequencing. Though most heat-resistance mutations were

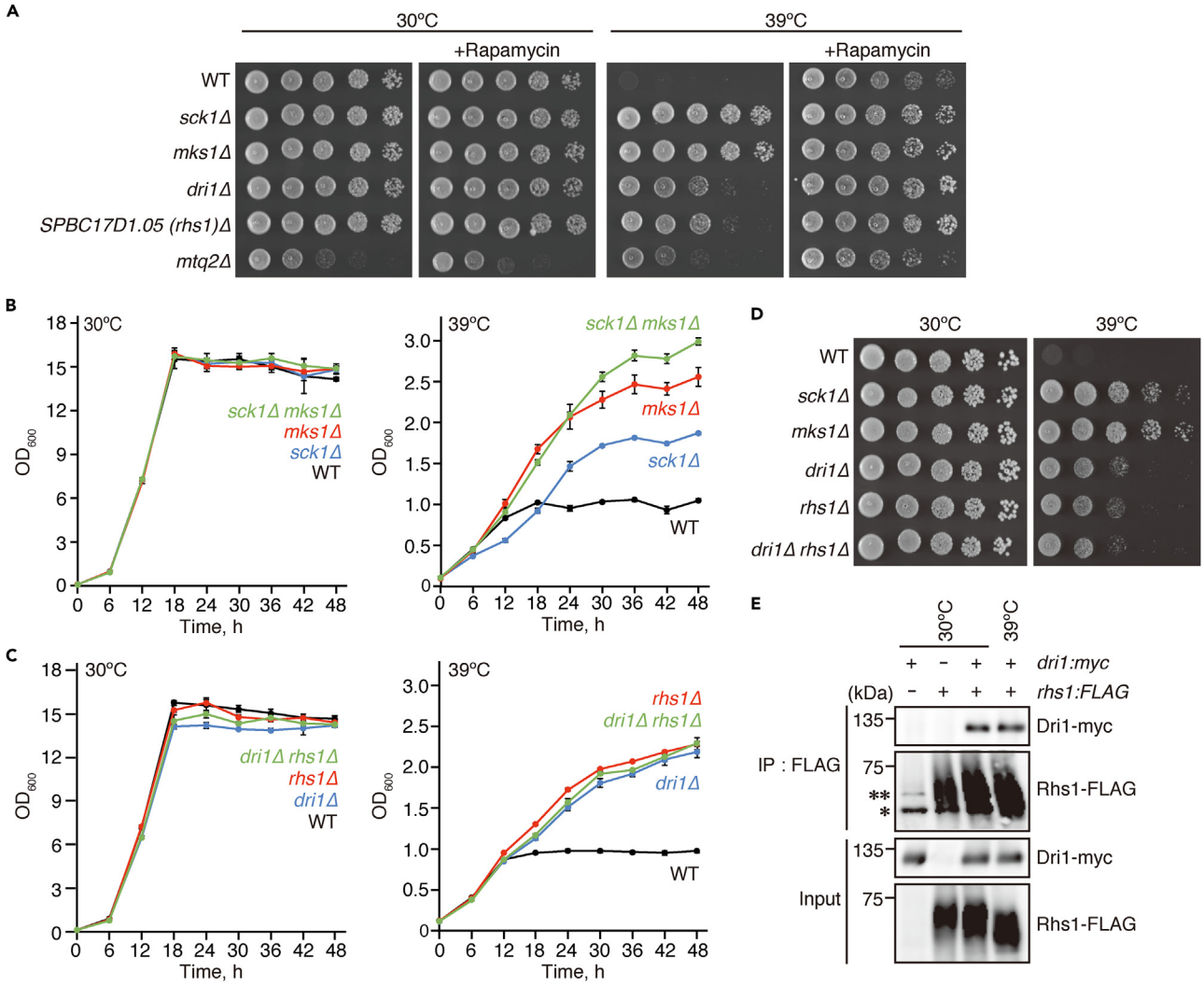

Figure 3. Identification of genes that suppress cellular growth at high temperatures

(A) Isolated gene deletion mutants that exhibit growth at high temperatures. The indicated null mutants were grown in YES medium at 30°C. Their growth in the presence and absence of rapamycin (100 ng/mL) was tested at 30°C and 39°C by spotting serial dilutions of their cultures on YES agar plates.

(B) Sck1 and Mks1 function independently to inhibit cell growth at high temperatures. Wild-type (WT) and the indicated mutant cells were cultured in YES medium at 30°C. At time 0, the culture concentration was adjusted to $OD_{600} = 0.1 \pm 0.02$, and their growth at 30°C and 39°C was monitored by measuring OD_{600} every 6 h. Data are presented as means ± SD from three independent experiments.

(C and D) Dri1 and Rhs1 function in the same pathway. (C) The growth kinetics of indicated mutant strains were measured as in (B). (D) The indicated mutant strains were grown in YES medium at 30°C, and their serial dilutions were spotted onto YES agar plates for growth assay at 30°C and 39°C.

(E) Dri1 physically interacts with Rhs1. Strains expressing Rhs1-FLAG and Dri1-*myc* individually or simultaneously were grown in YES medium at 30°C and 39°C, and the cell lysate was subjected to immunoprecipitation using anti-FLAG affinity beads (IP: FLAG). The samples were analyzed by anti-FLAG and anti-*myc* immunoblotting. Single and double asterisks indicate immunoglobulin heavy chains and a non-specific protein recognized by the anti-FLAG antibody, respectively. See also Figures S3 and S4.

found in the *sck1* or *dri1* genes, whose deletion also allows cell growth at 39°C (Figure 3A), one mutant carried a single nucleotide substitution in *rad24*, a gene encoding a 14-3-3 protein (Table S1). This mutation is predicted to replace Glu-185 with valine in Rad24, and the identical *rad24-E185V* mutation introduced to a wild-type strain by site-directed mutagenesis confirmed its ability to allow cell growth at 39°C (Figure 4A). On the other hand, the *rad24* (*rad24Δ*) null mutant exhibited little growth at 39°C while growing better than wild-type cells at 38°C. This result suggests that Rad24 is inhibitory to high-temperature growth. Importantly, the *rad24Δ mutation* slightly compromised cell proliferation even at 30°C, whereas *rad24-E185V* did not (Figure 4A). Therefore, *rad24-E185V* may be a partial loss-of-function mutation, conferring better growth than *rad24Δ* from 30°C to 39°C. It should also be noted that, in the presence of rapamycin, both *rad24-E185V* and *rad24Δ* cells did not grow as much as wild-type cells at 39°C (Figure 4A), implying a role of Rad24 in the rapamycin-induced heat resistance.

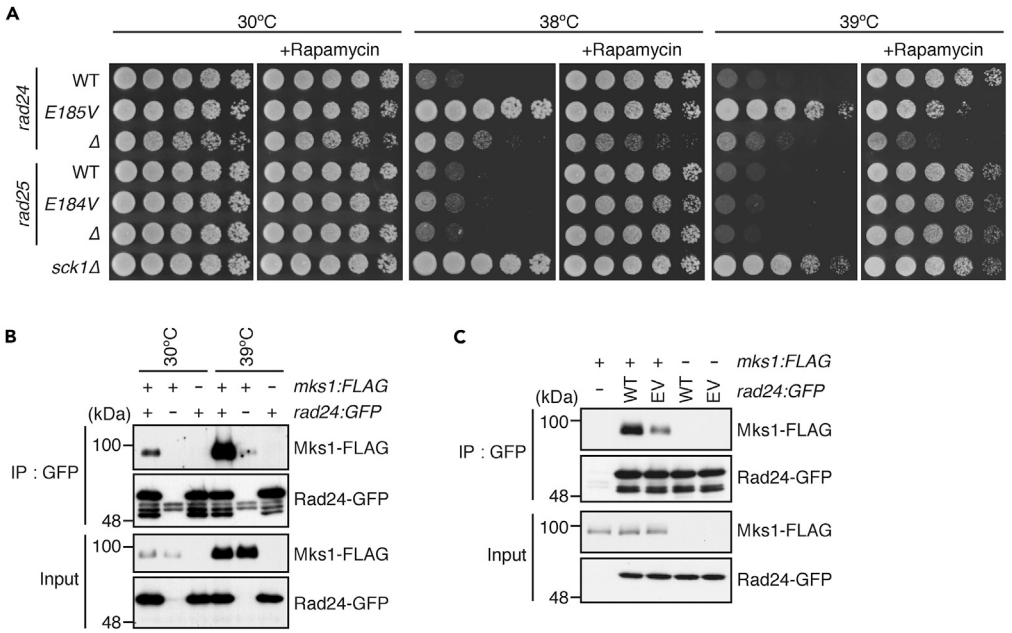

Figure 4. The *rad24-E185V* mutation, which compromises the Rad24-Mks1 interaction, confers heat resistance on *S. pombe* cells

(A) The *rad24-E185V* mutation confers heat resistance on fission yeast cells. The indicated strains were cultured at 30°C. Their growth in the presence and absence of rapamycin (100 ng/mL) was tested at indicated temperatures by spotting serial culture dilutions on YES agar plates.

(B) Mks1 physically interacts with Rad24. Strains expressing Mks1-FLAG and Rad24-GFP individually or simultaneously were grown in YES medium at 30°C and sifted to 39°C. After 2-h incubation at 39°C, the cell lysate was prepared, and Rad24-GFP was immunopurified using the antibodies against GFP (IP: GFP). Co-purified Mks1-FLAG was analyzed by immunoblotting.

(C) The *rad24-E185V* mutation compromises the interaction of Rad24 with Mks1. *mks1-FLAG* cells expressing either Rad24 or Rad24-E185V tagged with GFP were grown, and their cell lysate was subjected to immunoprecipitation followed by immunoblotting as in (B). See also Figure S4 and Table S1.

Glu-185 in Rad24 is conserved in the *S. pombe* 14-3-3 protein paralog Rad25 as Glu-184 (Figure S5). In contrast to the *rad24* mutants, both *rad25-E184V* and *rad25Δ* mutants failed to grow at 38°C and 39°C (Figure 4A), suggesting little or no contribution of Rad25 to the growth regulation under high-temperature conditions.

Budding yeast Mks1 physically interacts with Bmh1, a 14-3-3 protein orthologous to fission yeast Rad24.[41] As our study in fission yeast identified Mks1 and Rad24 as negative regulators of high-temperature growth, we examined the physical interaction between Mks1 and Rad24. Immunoprecipitation of Rad24 tagged with the green fluorescent protein (GFP) resulted in co-purification of the FLAG-tagged Mks1 protein at both 30°C and 39°C (Figure 4B). A less amount of Mks1 was co-purified with Rad24-E185V than with the wild-type Rad24 protein (Figure 4C). These results indicate that, like its ortholog in budding yeast, fission yeast Mks1 interacts with Rad24 and that their interaction is compromised by the *rad24-E185V* mutation.

The Mks1 protein is phosphorylated in a TORC1-dependent manner and accumulates in cells exposed to high temperatures

In the experiments shown in Figure 4B, we noticed that the amount of Mks1 in cells incubated at 39°C was significantly higher than that at 30°C, resulting in more Mks1 co-purified with Rad24 at 39°C. We confirmed that the Mks1 protein accumulated after the temperature shift from 30°C to 39°C and that rapamycin further promoted the accumulation (Figure 5A); even at 30°C, rapamycin can induce the accumulation of Mks1 (Figure S6A). On the other hand, the *mks1*$^{+}$ transcript did not significantly increase even after 4-h incubation at 39°C (Figure 5B), in contrast to the HSP genes such as *hsp16*$^{+}$.[45] Thus, the accumulation of Mks1 at high temperatures does not appear to be due to the transcriptional regulation of *mks1*$^{+}$. In addition, we observed a significantly elevated level of the Mks1 protein in the *mts2-1* background, a temperature-sensitive, hypomorphic allele of a 26S proteasome subunit,[61] even at the permissive temperature (Figure 5C). It is likely that proteasomal degradation regulates the cellular level of Mks1.

It was previously observed in budding yeast that the 14-3-3 protein Bmh1 binds to Mks1 and protects it from proteasomal degradation.[63] We therefore examined the cellular level of fission yeast Mks1 in the *rad24* mutants. As in wild-type cells, no accumulation of Mks1 was observed at 30°C in both *rad24Δ* and *rad24-E185V* mutants (Figure S6B). In addition, the accumulation of Mks1 after the temperature shift to 39°C was not notably affected by the *rad24* mutations when compared to the wild type. Thus, the 14-3-3 protein Rad24 does not have a major regulatory role in the proteasomal degradation of fission yeast Mks1.

The observed effect of rapamycin on the Mks1 protein level implies that TORC1 contributes to the regulation of Mks1, including its proteasomal degradation (Figures 5A and 5C). Several independent phosphoproteomic studies identified multiple phosphorylated

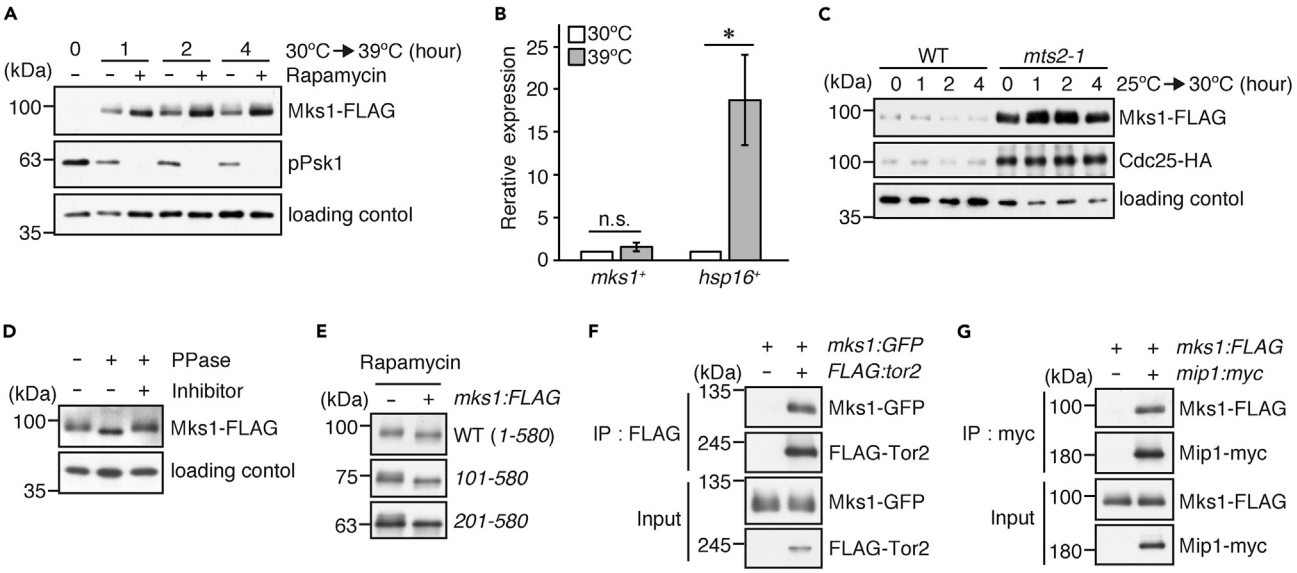

Figure 5. Cellular Mks1 protein, which is phosphorylated by TORC1, accumulates upon heat stress by attenuation of its proteasomal degradation

(A) Heat stress induces the accumulation of Mks1, which is further enhanced by rapamycin. Cells were grown in YES medium at 30°C and shifted to 39°C in the presence and absence of 200 ng/mL rapamycin. Their cell lysate was probed with anti-FLAG and anti-Spc1 (loading control) antibodies.

(B) Heat stress does not significantly change the transcription of the *mks1*$^{+}$ gene. The mRNA expression of *mks1*$^{+}$ and *hsp16*$^{+}$ was examined by qRT-PCR using cells grown in YES medium at 30°C and 39°C for 4 h. The expression level of each gene is presented as a value relative to that at 30°C. Bars indicate ± SD from two independent experiments in triplicate. *$p < 0.05$; n.s., not significant, compared to the mRNA expression at 30°C using Student's *t* test.

(C) The protein accumulation of Mks1 in the *mts2-1* mutant. Wild-type (WT) and *mts2-1* mutant cells were grown in YES medium at 25°C and shifted to 30°C. Cells were harvested at indicated time points, and their cell lysate was subjected to immunoblotting using anti-FLAG, anti-HA, and anti-Spc1 (loading control) antibodies. Cdc25, known to accumulate in the *mts2-1* mutant,[62] was utilized as a positive control.

(D) Mks1 is a phosphoprotein. Cell lysate prepared from a strain expressing FLAG-tagged Mks1 was treated with lambda phosphatase (PPase) in the presence or absence of phosphatase inhibitor and subjected to immunoblotting as in (A).

(E) Mks1 is phosphorylated in a manner dependent on TORC1. Cells expressing the indicated FLAG-tagged Mks1 proteins were grown in YES medium at 30°C and shifted to 39°C in the presence and absence of 200 ng/mL rapamycin. Their cell lysate was probed as in (A). Note that as rapamycin induces the Mks1 protein accumulation, the protein loading amount between rapamycin-treated and -untreated samples was adjusted to obtain comparable signals of Mks1.

(F and G) Physical interaction between TORC1 and Mks1. Strains expressing Mks1-GFP and FLAG-Tor2 (F), or Mks1-FLAG and Mip1-myc (G) individually or simultaneously were grown in YES medium at 30°C and sifted to 39°C. After 2-h incubation at 39°C, FLAG-Tor2 (F) or Mip1-myc (G) was immunopurified from cell lysate, and co-purified Mks1 was analyzed by immunoblotting. See also Figure S5 and Tables S2–S4.

serine/threonine residues in Mks1.[64–68] Indeed, phosphatase treatment altered the electrophoretic mobility of the Mks1 protein, confirming that Mks1 is a phosphoprotein (Figure 5D). In addition, the function of budding yeast Mks1 is believed to be regulated by TORC1-dependent phosphorylation.[37,41] We thus tested whether Mks1 is phosphorylated in a manner dependent on TORC1. The electrophoretic mobility of the Mks1 protein increased in the presence of rapamycin, particularly when its N-terminal 100 residues (101–580) or 200 residues (201–580) were deleted (Figure 5E). Moreover, in immunoprecipitation experiments, Mks1 was co-purified with Tor2 as well as Mip1, both of which are the TORC1 components (Figures 5F and 5G). These results suggest that fission yeast Mks1 is a direct substrate of TORC1. As Mks1 and Sck1 function in parallel (Figure 3B), it is likely that TORC1 phosphorylation controls these two factors independently in the negative regulation of high-temperature growth. Indeed, the growth of the *mks1Δ* strain at 39°C was further promoted in the presence of rapamycin, which suppresses Sck1 activity (Figure S6C).

14-3-3 proteins are known to preferentially bind the phosphorylated ligand proteins.[69] To assess the possibility that the TORC1-dependent phosphorylation of Mks1 promotes the Mks1-Rad24 association, their co-precipitation experiments were performed using cells treated with rapamycin. Consistent with the experiment shown in Figure S6A, rapamycin promoted Mks1 accumulation, which resulted in an increased amount of Mks1 co-purified with Rad24 (Figure S6D), suggesting that the TORC1-dependent phosphorylation of Mks1 is not required for its interaction with Rad24.

Budding yeast Mks1 negatively regulates a set of genes involved in lysine biosynthesis and the TCA cycle.[37–39,41] Our gene expression profiling analysis by RNA sequencing (RNA-seq) revealed that the *mks1Δ* mutation up- and downregulates 10 and 32 genes, respectively, which do not include the lysine biosynthetic and TCA cycle genes (Table S2). Thus, the function of Mks1 in gene regulation may not be conserved between budding and fission yeasts. A gene ontology (GO) analysis for molecular functions found that the most upregulated genes are annotated as "RNA binding," while the downregulated genes include those encoding proteins with enzymatic activities, such as beta-glucosidase and carbamoyl-phosphate synthase (Figure S6E). We also performed transcriptomic analysis of the rapamycin-treated

wild-type and *sck1Δ* strains (Tables S3 and S4). Among 82 genes downregulated in the presence of rapamycin, about a half are genes encoding ribosomal proteins (Figure S6F), consistent with the previous observations that suppression of TORC1 activity results in the reduction of ribosomal protein expression.[70,71] Interestingly, the 13 genes suppressed by rapamycin treatment are also downregulated in *mks1Δ* cells (Figure S6G). On the other hand, no significant enrichment of the GO functions was found in the 13 genes upregulated in the presence of rapamycin. In contrast to the *mks1Δ* mutation and rapamycin treatment, the *sck1Δ* mutation affected the expression of only a few genes (Table S4); Sck1 may not control cellular high-temperature growth through the transcription of genes involved in a certain cellular process.

Mks1 has a conserved C-terminal motif required for the suppression of cell growth at high temperatures

As described earlier, Mks1 interacts with the 14-3-3 protein Rad24, of which mutation *rad24-E185V* compromises their interaction and induces cellular heat resistance (Figure 4). Therefore, we further delved into the Mks1-Rad24 interaction and its role in heat-resistant cell growth. To determine the Rad24-binding region within Mks1, we repeated the Rad24 immunoprecipitation assays with fission yeast strains expressing a series of truncated Mks1 proteins. Truncation of the N-terminal 300 residues of Mks1 (301–580) abrogated its interaction with Rad24, whereas Mks1(101–580) and Mks1(201–580) were found to associate with Rad24 (Figure 6A). We also tested the mutant Mks1 proteins truncated from the C terminus and found that Mks1(1–280) interacted with Rad24, implying that residues 201–280 of Mks1 are involved in the interaction with Rad24. As shown in Figure 6B, a mutant strain expressing Mks1(301–580) that cannot interact with Rad24 exhibited moderate cell growth at 39°C, whereas cells expressing the full length, 101–580, or 201–580 of Mks1 failed to grow at 39°C. These observations are consistent with the idea that the Mks1-Rad24 interaction plays a role in the negative regulation of high-temperature growth.

Interestingly, strains expressing the C-terminally truncated Mks1 proteins, such as Mks1(1–480) that can bind Rad24 (Figure 6A), showed significant growth at 39°C (Figure 6B), suggesting that the C-terminal region of Mks1 is essential in suppressing growth at high temperatures. We noticed that residues 520–539 within this region are highly conserved among the Mks1 orthologs in several fungi, including *Schizosaccharomyces japonicus*, *Aspergillus nidulans*, and *Neurospora crassa*, but not in *S. cerevisiae* (Figure 6C). Thus, we next examined whether this conserved 20-residue sequence is required for the Mks1 function. Cells expressing the C-terminally truncated Mks1(1–510) that lacks this sequence stretch grew at 39°C, like the *mks1Δ* mutant (Figure 6D). In contrast, the Mks1(1–550) protein, which retains the conserved stretch, was capable of suppressing cell growth at this temperature. We also constructed a strain expressing Mks1 without this sequence motif, Mks1(Δ520–539), and the mutant strain was found to exhibit a *mks1Δ*-like phenotype at 39°C (Figure 6D). These results strongly suggest that the conserved C-terminal motif of Mks1 (Figure 6C) is critical for the Mks1 function.

To further characterize this conserved C-terminal motif of Mks1, we constructed a series of alanine-substitution mutants, in which the two successive residues within this region were replaced with alanine at a time. While the temperature sensitivity of the *mks1-RD530.531AA* and *-QK538.539AA* mutants was comparable to that of the wild-type strain, the other *mks1* alanine mutants showed significant growth at 39°C (Figure 6E). As expected, the Mks1-Rad24 interaction was not significantly affected by these alanine substitutions (Figure S7), confirming that the Mks1 defects caused by these C-terminal mutations are independent of the Mks1-Rad24 interaction.

Altogether, these results strongly suggest that Mks1 has a conserved C-terminal motif essential for its function in suppressing cellular growth at high temperatures. The Mks1 function is also modulated by the 14-3-3 protein Rad24, which interacts with residues 201–280 of Mks1.

DISCUSSION

Increasing concerns over climate warming[72] include how higher ambient temperatures affect living organisms and their ecosystems. A recent study indicates that the rate of heat death in diverse ectotherms is extremely temperature-sensitive and doubles for every 1°C rise.[73] Such acute temperature sensitivity is also observed in fission yeast cells under stressful temperatures; even a slight temperature increase from 37°C results in dramatically compromised proliferation and survival (Figure 1). In this study, we have discovered that the thermal limit of fission yeast growth is significantly extended by rapamycin, a specific inhibitor of TORC1.

TORC1, a well-known growth-promoting factor that potentiates anabolic processes such as protein synthesis, has turned out to be a suppressor of proliferation at high temperatures, most likely through the Sck1 kinase (Figures 1 and 2). A previous study in budding yeast found that the protein aggregation induced by arsenite attenuates cell growth and that this cytotoxic effect is suppressed by blocking the accumulation of protein aggregates with cycloheximide, an inhibitor of protein translation.[74] It is therefore plausible that the downregulation of protein synthesis by TORC1 inhibition results in less heat stress-induced protein aggregation, enabling cells to proliferate at high temperatures. However, a recent study indicates that the rate of protein synthesis is not significantly affected by the triple deletion of the AGC-family kinases Psk1, Sck1, and Sck2 in fission yeast.[75] Moreover, the suppression of TORC1 activity by rapamycin was reported to have little effect on global translation in this organism.[71] Thus, the enhanced high-temperature growth by the *sck1Δ* mutation or TORC1 inhibition may be independent of protein synthesis, and the proteotoxic stress may not be a major cause of the growth arrest at temperatures marginally above 37°C. Consistent with this idea, rapamycin, as well as the *sck1Δ* mutation, promotes high-temperature cell growth without the induction of HSPs such as Hsp16 (Figures S1B and S3A).

It was unexpected that the thermal limit of fission yeast growth is dictated by an intrinsic cellular mechanism, TORC1-Sck1 signaling, rather than the level of heat injury that brings about physiological collapse. Moreover, the finding that the deletion of the *sck1*$^{+}$ gene unleashes cell proliferation above 38°C implied that there may be additional genes inhibitory to high-temperature growth, including the one encoding the unknown substrate of the Sck1 kinase. Therefore, we screened a haploid null mutant library of *S. pombe* and identified four more genes whose null mutants exhibit growth even at 39°C (Figures 3 and 6F). Genetic analysis suggested that all those genes function independently of Sck1 to negatively regulate cell proliferation at high temperatures. The genes that we identified include a protein with some homology to budding

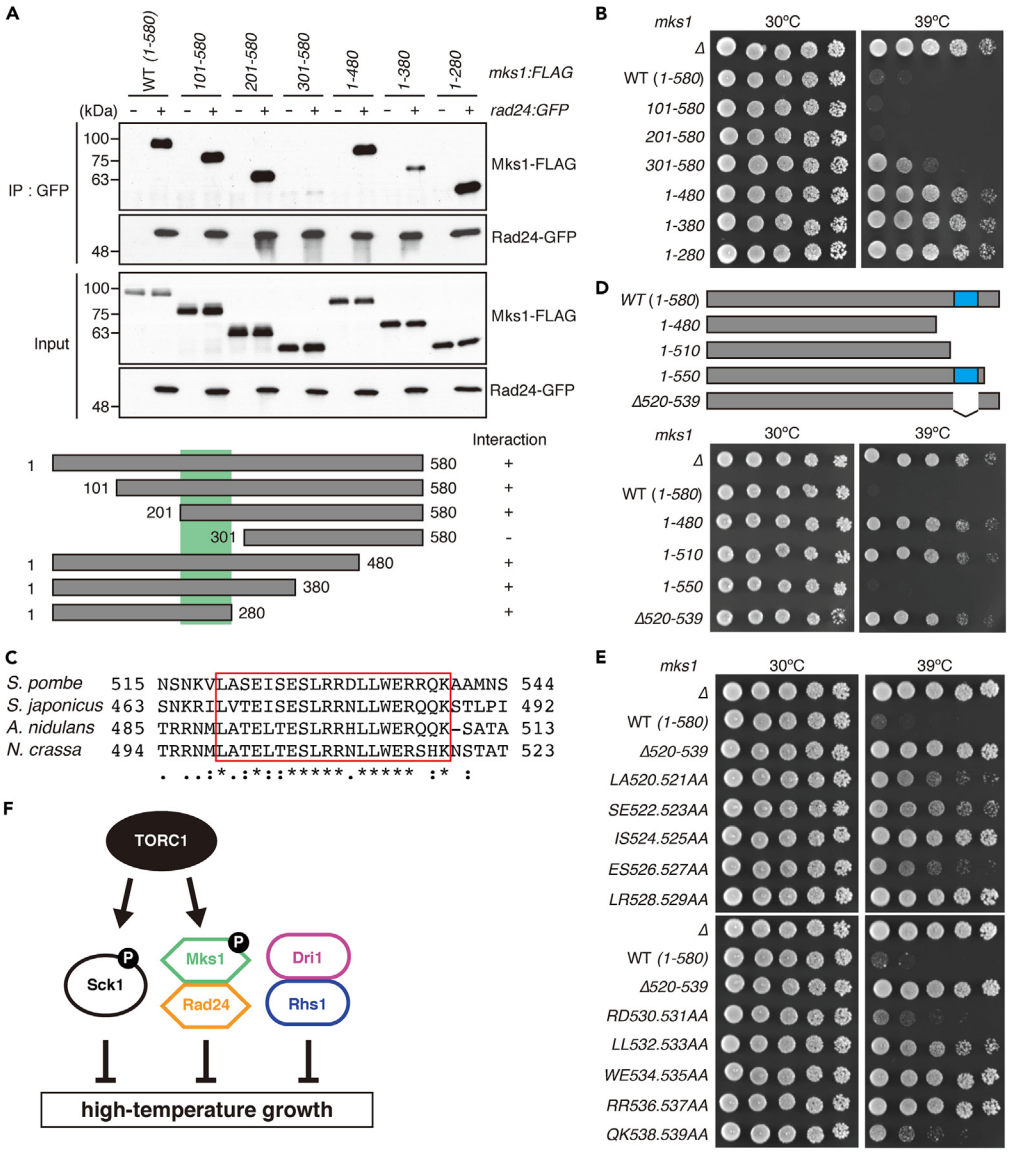

Figure 6. The C-terminal conserved region of Mks1 is indispensable for the suppression of high-temperature growth

(A) The interaction of Rad24 with various truncated Mks1 fragments. *rad24:GFP* cells expressing various Mks1 fragments were cultured in YES medium at 30°C and sifted to 39°C. After 2-h incubation at 39°C, their cell lysate was subjected to immunoprecipitation using the anti-GFP antibodies (IP: GFP), and co-purified Mks1-FLAG was analyzed by immunoblotting. A green box in the schematic diagram of the Mks1 fragments indicates the region required for the Mks1-Rad24 interaction.

(B) The growth of the strains expressing the various Mks1 fragments at high temperatures. The indicated *mks1* mutant strains were grown in YES medium at 30°C, and their serial dilutions were spotted onto YES agar plates for growth assay at 30°C and 39°C.

(C) Amino acid sequence alignment of the C-terminal conserved region of Mks1 in *S. pombe*, *S. japonicus*, *A. nidulans*, and *N. crassa*. The sequence alignment was performed using the CLUSTALW program (https://www.genome.jp/tools-bin/clustalw). Asterisks, identical amino acids; single and double dots, weakly and strongly similar amino acids, respectively. The conserved sequence stretches are shown in a red box.

(D and E) The C-terminal conserved region of Mks1 is indispensable for its function of suppressing cell growth at high temperatures. The growth of the indicated *mks1* mutant cells at 39°C was examined as in (B). A blue box in a schematic diagram of the Mks1 fragments in (D) indicates the conserved C-terminal region.

(F) A model illustrating the negative regulation of cell growth under heat stress in fission yeast. See also Figure S7.

yeast Mks1, which physically interacts with the 14-3-3 protein, Bmh1.[41] We found that fission yeast Mks1 also binds to the 14-3-3 protein Rad24, whose Glu-185-to-Val mutation was isolated during our screen for spontaneous heat-resistant mutants (Figure 4). 14-3-3 proteins regulate various cellular processes through interaction with a diverse array of proteins.[69,76] Interestingly, Glu-185 in Rad24 is highly conserved among 14-3-3 proteins in divergent eukaryotic species,[77] and this glutamate residue directly binds some of the 14-3-3 protein ligands.[78,79] Indeed, the

rad24-E185V mutation attenuates the interaction of Rad24 with Mks1, implying the involvement of Rad24 Glu-185 in the Rad24-Mks1 complex formation.

The Mks1 protein accumulates in cells exposed to high temperatures (Figure 5A), and the *mks1Δ* mutation confers heat resistance on fission yeast cells (Figure 3A). However, the Mks1 accumulation *per se* may not be responsible for the growth inhibition at high temperatures, as rapamycin promotes both Mks1 accumulation and cell proliferation above the normal permissive temperatures. Notably, we detected the TORC1-dependent phosphorylation of Mks1 (Figure 5E), although the phosphorylation does not appear to affect the Mks1-Rad24 interaction (Figure S6D). It is conceivable that suppression of TORC1 activity by rapamycin results in the accumulation of an unphosphorylated, inactive form of Mks1, which is incapable of inhibiting cell growth at high temperatures. However, in the presence of TORC1 activity, phosphorylated Mks1 accumulates under high-temperature conditions and, together with Rad24, restricts cellular proliferation (Figure 4).

Our screen of the mutant library also led to the identification of Dri1 as a negative regulator of cell proliferation at high temperatures (Figure 3A). It was recently reported that Dri1 mediates heterochromatin assembly, which is compromised when Dri1 is tagged by the green fluorescent protein at the C terminus (Dri1-GFP).[55] On the other hand, unlike the *dri1Δ* mutant, the temperature sensitivity of the Dri1-GFP strain constructed in our laboratory is comparable to that of the wild-type strain (Figure S8); thus, suppression of the high-temperature growth by Dri1 appears to be independent of its function in heterochromatin assembly. Indeed, such dual functionality of Dri1 may be regulated by its binding partners. Dri1 interacts with Dpb4, a subunit of DNA polymerase epsilon, to regulate heterochromatin assembly,[55] whereas we found that Rhs1 associates with Dri1 and suppresses high-temperature growth (Figures 3C and 3D).

In summary, we have found that fission yeast is capable of growing at temperatures higher than previously thought and that such high-temperature growth is under negative regulation by cellular mechanisms, including TORC1-Sck1 (Figure 6F). It is of great interest to understand why the thermal limit of fission yeast is set below the temperatures deleterious to cell physiology. Spontaneous mutation rates are known to rise with temperature increases in various model organisms[80–82]; thus, limiting high-temperature growth might contribute to genetic stability. There is also a possibility that expanded high-temperature tolerance compromises growth under other conditions.[58,59] We found that the *mtq2Δ* mutation can increase cellular thermotolerance, but the growth rate of the mutant strain is significantly reduced even at 30°C and 34°C (Figures 3A and S3A). Although the other genes we identified in this study did not significantly affect cellular growth under the conditions we tested, their loss could have trade-offs under specific environments.

Another significant question is whether similar negative controls, rather than direct heat damage to cellular components, determine the thermal limits in other unicellular organisms and cells in multicellular organisms. Mutations that increase cellular thermotolerance have also been isolated through experimental evolution in the budding yeast *S. cerevisiae*, which is only distantly related to *S. pombe*.[81] Curiously, most of the inhibitors of high-temperature growth that we identified in this study, including TORC1, are conserved among eukaryotic species. We expect that further analyses of those factors in fission yeast and other eukaryotes will provide a novel insight into the determinants of the cellular thermal limit, which governs phenomena in multicellular systems under stressful heat, including climate warming.

Limitation of the study

In this study, we screened an *S. pombe* haploid null mutant library for mutants that can grow at 39°C. This library covers approximately 3,400 nonessential genes; however, the screen did not evaluate the functions of genes essential for cell viability in the negative regulation of cell proliferation at high temperatures. For example, our library screens failed to identify the essential TORC1 components, such as Tor2 and Mip1, which we have found suppress cellular growth at high temperatures. Thus, our study may not have comprehensively identified high-temperature growth regulators; additional factors need to be sought to understand better the genetic network that controls the growth of fission yeast at high temperatures.

STAR★METHODS

Detailed methods are provided in the online version of this paper and include the following:

- KEY RESOURCES TABLE
- RESOURCE AVAILABILITY
  - Lead contact
  - Materials availability
  - Data and code availability
- EXPERIMENTAL MODEL AND STUDY PARTICIPANT DETAILS
  - Fission yeast strains and general methods
- METHOD DETAILS
  - *S. pombe* growth assay
  - Cell viability assay
  - Immunoblotting
  - *S. pombe* deletion library screen
  - Immunoprecipitation assay
  - Phosphatase treatment
  - Isolation of spontaneous mutants that can grow at high temperatures

- Whole-genome sequencing and data analysis
- RNA extraction, RT-qPCR and RNA-seq

- QUANTIFICATION AND STATISTICAL ANALYSIS

SUPPLEMENTAL INFORMATION

Supplemental information can be found online at https://doi.org/10.1016/j.isci.2023.108777.

ACKNOWLEDGMENTS

This study was supported by research grants to K.S. from the Ohsumi Frontier Science Foundation and Takeda Science Foundation, to Y.M. from the Institute for Fermentation, Osaka (IFO) and Sumitomo Foundation, and to K.O. from the Japan Agency for Medical Research and Development (AMED) (JP20wm0325003), Japan Science and Technology Agency (JST) CREST (JPMJCR18S3), and AMED-CREST (JP23gm161000). This work was also supported by the Japan Society for the Promotion of Science (JSPS) KAKENHI grants (19K06564 and 22K06145 to Y.M., 19H03224 to K.S., 20K06485 to Y.N., 19K16070 and 23K04984 to A.H.O.). F.S. was supported by the Graduate Student Scholarships from the Panasonic Corporation and the Sato Yo International Scholarship Foundation. We thank A Higuchi for technical assistance and D Watanabe for discussion. We are also grateful to T Toda and M Yukawa for sharing unpublished data and strains, and to T Matsumoto and the NBRP Japan for strains.

AUTHOR CONTRIBUTIONS

Y.M., K.O., and K.S. designed research; Y.M., F.M., Y.N., J.X.S., S.Y., F.S., Y.I., A.H.O., M.T., S.K., and Y.A. performed research; Y.M., F.M., Y.N., J.X.S., F.S., Y.I., A.H.O., and M.T. analyzed data; and Y.M. and K.S. wrote the paper.

DECLARATION OF INTERESTS

The authors declare no competing interests.

INCLUSION AND DIVERSITY

We support inclusive, diverse, and equitable conduct of research.

Received: May 25, 2023
Revised: October 12, 2023
Accepted: December 22, 2023
Published: December 26, 2023

REFERENCES

1. Mogk, A., Bukau, B., and Kampinga, H.H. (2018). Cellular Handling of Protein Aggregates by Disaggregation Machines. Mol. Cell *69*, 214–226.
2. Tyedmers, J., Mogk, A., and Bukau, B. (2010). Cellular strategies for controlling protein aggregation. Nat. Rev. Mol. Cell Biol. *11*, 777–788.
3. Richter, K., Haslbeck, M., and Buchner, J. (2010). The Heat Shock Response: Life on the Verge of Death. Mol. Cell *40*, 253–266.
4. Verghese, J., Abrams, J., Wang, Y., and Morano, K.A. (2012). Biology of the Heat Shock Response and Protein Chaperones: Budding Yeast (Saccharomyces cerevisiae) as a Model System. Microbiol. Mol. Biol. Rev. *76*, 115–158.
5. Gidalevitz, T., Prahlad, V., and Morimoto, R.I. (2011). The stress of protein misfolding: From single cells to multicellular organisms. Cold Spring Harb. Perspect. Biol. *3*, a009704–a009718.
6. Radwan, M., Wood, R.J., Sui, X., and Hatters, D.M. (2017). When proteostasis goes bad: Protein aggregation in the cell. IUBMB Life *69*, 49–54.
7. Zoncu, R., Efeyan, A., and Sabatini, D.M. (2011). mTOR: from growth signal integration to cancer, diabetes and ageing. Nat. Rev. Mol. Cell Biol. *12*, 21–35.
8. Loewith, R., Jacinto, E., Wullschleger, S., Lorberg, A., Crespo, J.L., Bonenfant, D., Oppliger, W., Jenoe, P., and Hall, M.N. (2002). Two TOR Complexes, Only One of which Is Rapamycin Sensitive, Have Distinct Roles in Cell Growth Control. Mol. Cell *10*, 457–468.
9. Wullschleger, S., Loewith, R., and Hall, M.N. (2006). TOR Signaling in Growth and Metabolism. Cell *124*, 471–484.
10. Saxton, R.A., and Sabatini, D.M. (2017). mTOR Signaling in Growth, Metabolism, and Disease. Cell *168*, 960–976.
11. González, A., and Hall, M.N. (2017). Nutrient sensing and TOR signaling in yeast and mammals. EMBO J. *36*, 397–408.
12. Bar-Peled, L., and Sabatini, D.M. (2014). Regulation of mTORC1 by amino acids. Trends Cell Biol. *24*, 400–406.
13. Kim, J., and Guan, K.L. (2019). mTOR as a central hub of nutrient signalling and cell growth. Nat. Cell Biol. *21*, 63–71.
14. Sancak, Y., Peterson, T.R., Shaul, Y.D., Lindquist, R.A., Thoreen, C.C., Bar-Peled, L., and Sabatini, D.M. (2008). The Rag GTPases Bind Raptor and Mediate Amino Acid Signaling to mTORC1. Science *320*, 1496–1501.
15. Yang, H., Jiang, X., Li, B., Yang, H.J., Miller, M., Yang, A., Dhar, A., and Pavletich, N.P. (2017). Mechanisms of mTORC1 activation by RHEB and inhibition by PRAS40. Nature *552*, 368–373.
16. Burnett, P.E., Barrow, R.K., Cohen, N.A., Snyder, S.H., and Sabatini, D.M. (1998). RAFT1 phosphorylation of the translational regulators p70 S6 kinase and 4E-BP1. Proc. Natl. Acad. Sci. USA *95*, 1432–1437.
17. Ma, X.M., and Blenis, J. (2009). Molecular mechanisms of mTOR-mediated translational control. Nat. Rev. Mol. Cell Biol. *10*, 307–318.
18. Fumagalli, S., and Pende, M. (2022). S6 kinase 1 at the central node of cell size and ageing. Front. Cell Dev. Biol. *10*, 949196–949212.
19. Musa, J., Orth, M.F., Dallmayer, M., Baldauf, M., Pardo, C., Rotblat, B., Kirchner, T., Leprivier, G., and Grünewald, T.G.P. (2016). Eukaryotic initiation factor 4E-binding protein 1 (4E-BP1): a master regulator of mRNA translation involved in tumorigenesis. Oncogene *35*, 4675–4688.
20. Morozumi, Y., and Shiozaki, K. (2021). Conserved and Divergent Mechanisms That Control TORC1 in Yeasts and Mammals. Genes *12*, 88.
21. Alvarez, B., and Moreno, S. (2006). Fission yeast Tor2 promotes cell growth and represses cell differentiation. J. Cell Sci. *119*, 4475–4485.

22. Matsuo, T., Otsubo, Y., Urano, J., Tamanoi, F., and Yamamoto, M. (2007). Loss of the TOR Kinase Tor2 Mimics Nitrogen Starvation and Activates the Sexual Development Pathway in Fission Yeast. Mol. Cell Biol. *27*, 3154–3164.
23. Hayashi, T., Hatanaka, M., Nagao, K., Nakaseko, Y., Kanoh, J., Kokubu, A., Ebe, M., and Yanagida, M. (2007). Rapamycin sensitivity of the Schizosaccharomyces pombe tor2 mutant and organization of two highly phosphorylated TOR complexes by specific and common subunits. Gene Cell. *12*, 1357–1370.
24. Mach, K.E., Furge, K.A., and Albright, C.F. (2000). Loss of Rhb1, a Rheb-related GTPase in fission yeast, causes growth arrest with a terminal phenotype similar to that caused by nitrogen starvation. Genetics *155*, 611–622.
25. Urano, J., Comiso, M.J., Guo, L., Aspuria, P.J., Deniskin, R., Tabancay, A.P., Kato-Stankiewicz, J., and Tamanoi, F. (2005). Identification of novel single amino acid changes that result in hyperactivation of the unique GTPase, Rheb, in fission yeast. Mol. Microbiol. *58*, 1074–1086.
26. Uritani, M., Hidaka, H., Hotta, Y., Ueno, M., Ushimaru, T., and Toda, T. (2006). Fission yeast Tor2 links nitrogen signals to cell proliferation and acts downstream of the Rheb GTPase. Gene Cell. *11*, 1367–1379.
27. Chia, K.H., Fukuda, T., Sofyantoro, F., Matsuda, T., Amai, T., and Shiozaki, K. (2017). Ragulator and GATOR1 complexes promote fission yeast growth by attenuating TOR complex 1 through Rag GTPases. Elife *6*, e30880.
28. Fukuda, T., Sofyantoro, F., Tai, Y.T., Chia, K.H., Matsuda, T., Murase, T., Morozumi, Y., Tatebe, H., Kanki, T., and Shiozaki, K. (2021). Tripartite suppression of fission yeast TORC1 signaling by the GATOR1-Sea3 complex, the TSC complex, and Gcn2 kinase. Elife *10*, e60969.
29. Nakashima, A., Otsubo, Y., Yamashita, A., Sato, T., Yamamoto, M., and Tamanoi, F. (2012). Psk1, an AGC kinase family member in fission yeast, is directly phosphorylated and controlled by TORC1 and functions as S6 kinase. J. Cell Sci. *125*, 5840–5849.
30. Morozumi, Y., Hishinuma, A., Furusawa, S., Sofyantoro, F., Tatebe, H., and Shiozaki, K. (2021). Fission yeast TOR complex 1 phosphorylates Psk1 through an evolutionarily conserved interaction mediated by the TOS motif. J. Cell Sci. *134*, jcs258865.
31. Shinozaki-Yabana, S., Watanabe, Y., and Yamamoto, M. (2000). Novel WD-Repeat Protein Mip1p Facilitates Function of the Meiotic Regulator Mei2p in Fission Yeast.
32. Weisman, R., Choder, M., and Koltin, Y. (1997). Rapamycin specifically interferes with the developmental response of fission yeast to starvation. J. Bacteriol. *179*, 6325–6334.
33. Heitman, J., Movva, N.R., and Hall, M.N. (1991). Targets for cell cycle arrest by the immunosuppressant rapamycin in yeast. Science *253*, 905–909.
34. Takahara, T., and Maeda, T. (2012). TORC1 of fission yeast is rapamycin-sensitive. Gene Cell. *17*, 698–708.
35. Eskes, E., Deprez, M.-A., Wilms, T., and Winderickx, J. (2018). pH homeostasis in yeast; the phosphate perspective. Curr. Genet. *64*, 155–161.
36. Jazwinski, S.M., and Kriete, A. (2012). The Yeast Retrograde Response as a Model of Intracellular Signaling of Mitochondrial Dysfunction. Front. Physiol. *3*, 139–212.
37. Dilova, I., Chen, C.Y., and Powers, T. (2002). Mks1 in concert with TOR signaling negatively regulates RTG target gene expression in S. cerevisiae. Curr. Biol. *12*, 389–395.
38. Sekito, T., Liu, Z., Thornton, J., and Butow, R.A. (2002). RTG-dependent mitochondria-to-nucleus signaling is regulated by MKS1 and is linked to formation of yeast prion [URE3]. Mol. Biol. Cell *13*, 795–804.
39. Tate, J.J., Cox, K.H., Rai, R., and Cooper, T.G. (2002). Mks1p is required for negative regulation of retrograde gene expression in Saccharomyces cerevisiae but does not affect nitrogen catabolite repression-sensitive gene expression. J. Biol. Chem. *277*, 20477–20482.
40. Dilova, I., Aronova, S., Chen, J.C.Y., and Powers, T. (2004). Tor signaling and nutrient-based signals converge on Mks1p phosphorylation to regulate expression of Rtg1p·Rtg3p-dependent target genes. J. Biol. Chem. *279*, 46527–46535.
41. Liu, Z., Sekito, T., Spírek, M., Thornton, J., and Butow, R.A. (2003). Retrograde signaling is regulated by the dynamic interaction between Rtg2p and Mks1p. Mol. Cell *12*, 401–411.
42. Otsubo, Y., Nakashima, A., Yamamoto, M., and Yamashita, A. (2017). TORC1-Dependent Phosphorylation Targets in Fission Yeast. Biomolecules *7*, 50.
43. Tang, C., Wei, J., Han, Q., Liu, R., Duan, X., Fu, Y., Huang, X., Wang, X., and Kang, Z. (2015). PsANT, the adenine nucleotide translocase of Puccinia striiformis, promotes cell death and fungal growth. Sci. Rep. *5*, 11241–11315.
44. Vairo, M.L.R. (1961). Methylene Blue Solutions for Staining Dead Yeast Cells. Stain Technol. *36*, 329–330.
45. Taricani, L., Feilotter, H.E., Weaver, C., and Young, P.G. (2001). Expression of hsp16 in response to nucleotide depletion is regulated via the spc1 MAPK pathway in Schizosaccharomyces pombe. Nucleic Acids Res. *29*, 3030–3040.
46. De Virgilio, C., Simmen, U., Hottiger, T., Boller, T., and Wiemken, A. (1990). Heat shock induces enzymes of trehalose metabolism, trehalose accumulation, and thermotolerance in Schizosaccharomyces pombe, even in the presence of cycloheximide. FEBS Lett. *273*, 107–110.
47. Shiozaki, K., Akhavan-Niaki, H., Mcgowan, C.H., and Russell, P. (1994). Protein Phosphatase 2C, Encoded by ptc1 + , Is Important in the Heat Shock Response of Schizosaccharomyces pombe. Mol. Cell Biol. *14*, 3742–3751.
48. Zuin, A., Carmona, M., Morales-Ivorra, I., Gabrielli, N., Vivancos, A.P., Ayté, J., and Hidalgo, E. (2010). Lifespan extension by calorie restriction relies on the Sty1 MAP kinase stress pathway. EMBO J. *29*, 981–991.
49. Costello, G., Rodgers, L., and Beach, D. (1986). Fission yeast enters the stationary phase G0 state from either mitotic G1 or G2. Curr. Genet. *11*, 119–125.
50. Weisman, R., Finkelstein, S., and Choder, M. (2001). Rapamycin Blocks Sexual Development in Fission Yeast through Inhibition of the Cellular Function of an FKBP12 Homolog. J. Biol. Chem. *276*, 24736–24742.
51. Nakashima, A., Sato, T., and Tamanoi, F. (2010). Fission yeast TORC1 regulates phosphorylation of ribosomal S6 proteins in response to nutrients and its activity is inhibited by rapamycin. J. Cell Sci. *123*, 777–786.
52. Ikai, N., Nakazawa, N., Hayashi, T., and Yanagida, M. (2011). The reverse, but coordinated, roles of Tor2 (TORC1) and Tor1 (TORC2) kinases for growth, cell cycle and separase-mediated mitosis in Schizosaccharomyces pombe. Open Biol. *1*, 110007.
53. Shetty, M., Noguchi, C., Wilson, S., Martinez, E., Shiozaki, K., Sell, C., Mell, J.C., and Noguchi, E. (2020). Maf1-dependent transcriptional regulation of tRNAs prevents genomic instability and is associated with extended lifespan. Aging Cell *19*, e13068.
54. Yukawa, M., Ohishi, M., Yamada, Y., and Toda, T. (2021). The putative rna-binding protein dri1 promotes the loading of kinesin-14/klp2 to the mitotic spindle and is sequestered into heat-induced protein aggregates in fission yeast. Int. J. Mol. Sci. *22*, 4795–4817.
55. Ban, H., Sun, W., Chen, Y.H., Chen, Y., and Li, F. (2021). Dri1 mediates heterochromatin assembly via RNAi and histone deacetylation. Genetics *218*, iyab032.
56. Bourgeois, G., Létoquart, J., van Tran, N., and Graille, M. (2017). Trm112, a protein activator of methyltransferases modifying actors of the eukaryotic translational apparatus. Biomolecules *7*, 7–19.
57. Lacoux, C., Wacheul, L., Saraf, K., Pythoud, N., Huvelle, E., Figaro, S., Graille, M., Carapito, C., Lafontaine, D.L.J., and Heurgué-Hamard, V. (2020). The catalytic activity of the translation termination factor methyltransferase Mtq2-Trm112 complex is required for large ribosomal subunit biogenesis. Nucleic Acids Res. *48*, 12310–12325.
58. Baker, E.P., Peris, D., Moriarty, R.V., Li, X.C., Fay, J.C., and Hittinger, C.T. (2019). Mitochondrial DNA and temperature tolerance in lager yeasts. Sci. Adv. *5*, eaav1869.
59. Caspeta, L., and Nielsen, J. (2015). Thermotolerant Yeast Strains Adapted by Laboratory Evolution Show Trade-Off at Ancestral Temperatures and Preadaptation to Other Stresses. mBio *6*, e00431.
60. Vo, T.V., Das, J., Meyer, M.J., Cordero, N.A., Akturk, N., Wei, X., Fair, B.J., Degatano, A.G., Fragoza, R., Liu, L.G., et al. (2016). A Proteome-wide Fission Yeast Interactome Reveals Network Evolution Principles from Yeasts to Human. Cell *164*, 310–323.
61. Gordon, C., McGurk, G., Dillon, P., Rosen, C., and Hastie, N.D. (1993). Defective mitosis due to a mutation in the gene for a fission yeast 26S protease subunit. Nature *366*, 355–357.
62. Frazer, C., and Young, P.G. (2012). Carboxy-terminal phosphorylation sites in Cdc25 contribute to enforcement of the DNA damage and replication checkpoints in fission yeast. Curr. Genet. *58*, 217–234.
63. Liu, Z., Spírek, M., Thornton, J., and Butow, R.A. (2005). A Novel Degron-mediated Degradation of the RTG Pathway Regulator, Mks1p, by SCF Grr1. Mol. Biol. Cell *16*, 4893–4904.
64. Tay, Y.D., Leda, M., Spanos, C., Rappsilber, J., Goryachev, A.B., and Sawin, K.E. (2019). Fission Yeast NDR/LATS Kinase Orb6 Regulates Exocytosis via Phosphorylation of the Exocyst Complex. Cell Rep. *26*, 1654–1667.e7.
65. Swaffer, M.P., Jones, A.W., Flynn, H.R., Snijders, A.P., and Nurse, P. (2018). Quantitative Phosphoproteomics Reveals the Signaling Dynamics of Cell-Cycle Kinases in

the Fission Yeast Schizosaccharomyces pombe. Cell Rep. *24*, 503–514.
66. Halova, L., Cobley, D., Franz-Wachtel, M., Wang, T., Morrison, K.R., Krug, K., Nalpas, N., Maček, B., Hagan, I.M., Humphrey, S.J., and Petersen, J. (2021). A TOR (target of rapamycin) and nutritional phosphoproteome of fission yeast reveals novel targets in networks conserved in humans. Open Biol. *11*, 200405.
67. Carpy, A., Krug, K., Graf, S., Koch, A., Popic, S., Hauf, S., and Macek, B. (2014). Absolute proteome and phosphoproteome dynamics during the cell cycle of Schizosaccharomyces pombe (fission yeast). Mol. Cell. Proteomics *13*, 1925–1936.
68. Kettenbach, A.N., Deng, L., Wu, Y., Baldissard, S., Adamo, M.E., Gerber, S.A., and Moseley, J.B. (2015). Quantitative Phosphoproteomics Reveals Pathways for Coordination of Cell Growth and Division by the Conserved Fission Yeast Kinase Pom1. Mol. Cell. Proteomics *14*, 1275–1287.
69. Morrison, D.K. (2009). The 14-3-3 proteins: integrators of diverse signaling cues that impact cell fate and cancer development. Trends Cell Biol. *19*, 16–23.
70. Powers, T., and Walter, P. (1999). Regulation of ribosome biogenesis by the rapamycin-sensitive TOR- signaling pathway in Saccharomyces cerevisiae. Mol. Biol. Cell *10*, 987–1000.
71. Rallis, C., Codlin, S., and Bähler, J. (2013). TORC1 signaling inhibition by rapamycin and caffeine affect lifespan, global gene expression, and cell proliferation of fission yeast. Aging Cell *12*, 563–573.
72. Seneviratne, S.I., Zhang, X., Adnan, M., Badi, W., Dereczynski, C., Di Luca, A., Ghosh, S., Iskandar, I., Kossin, J., Lewis, S., et al. (2021). Weather and Climate Extreme Events in a Changing Climate. In Climate Change 2021: The Physical Science Basis. Contribution of Working Group I to the Sixth Assessment Report of the Intergovernmental Panel on Climate Change (Cambridge University Press), pp. 1513–1766.
73. Jørgensen, L.B., Ørsted, M., Malte, H., Wang, T., and Overgaard, J. (2022). Extreme escalation of heat failure rates in ectotherms with global warming. Nature *611*, 93–98.
74. Jacobson, T., Navarrete, C., Sharma, S.K., Sideri, T.C., Ibstedt, S., Priya, S., Grant, C.M., Christen, P., Goloubinoff, P., and Tamás, M.J. (2012). Arsenite interferes with protein folding and triggers formation of protein aggregates in yeast. J. Cell Sci. *125*, 5073–5083.
75. Mak, T., Jones, A.W., and Nurse, P. (2021). The TOR-dependent phosphoproteome and regulation of cellular protein synthesis. EMBO J. *40*, e107911–e107919.
76. Fu, H., Subramanian, R.R., and Masters, S.C. (2000). 14-3-3 Proteins: Structure, Function, and Regulation. Annu. Rev. Pharmacol. Toxicol. *40*, 617–647.
77. Bridges, D., and Moorhead, G.B.G. (2005). 14-3-3 Proteins: a Number of Functions for a Numbered Protein. Sci. STKE *2005*, re10.
78. Alblova, M., Smidova, A., Docekal, V., Vesely, J., Herman, P., Obsilova, V., and Obsil, T. (2017). Molecular basis of the 14-3-3 protein-dependent activation of yeast neutral trehalase Nth1. Proc. Natl. Acad. Sci. *114*, E9811–E9820.
79. Edwards, M.R., Hoad, M., Tsimbalyuk, S., Menicucci, A.R., Messaoudi, I., Forwood, J.K., and Basler, C.F. (2020). Henipavirus W Proteins Interact with 14-3-3 To Modulate Host Gene Expression. J. Virol. *94*, e00373-20.
80. Chu, X.-L., Zhang, B.-W., Zhang, Q.-G., Zhu, B.-R., Lin, K., and Zhang, D.-Y. (2018). Temperature responses of mutation rate and mutational spectrum in an Escherichia coli strain and the correlation with metabolic rate. BMC Evol. Biol. *18*, 126.
81. Huang, C.-J., Lu, M.-Y., Chang, Y.-W., and Li, W.-H. (2018). Experimental Evolution of Yeast for High-Temperature Tolerance. Mol. Biol. Evol. *35*, 1823–1839.
82. Belfield, E.J., Brown, C., Ding, Z.J., Chapman, L., Luo, M., Hinde, E., van Es, S.W., Johnson, S., Ning, Y., Zheng, S.J., et al. (2021). Thermal stress accelerates Arabidopsis thaliana mutation rate. Genome Res. *31*, 40–50.
83. Tatebe, H., and Shiozaki, K. (2003). Identification of Cdc37 as a Novel Regulator of the Stress-Responsive Mitogen-Activated Protein Kinase. Mol. Cell Biol. *23*, 5132–5142.
84. Noguchi, C., Garabedian, M.V., Malik, M., and Noguchi, E. (2008). A vector system for genomic FLAG epitope-tagging in Schizosaccharomyces pombe. Biotechnol. J. *3*, 1280–1285.
85. Li, H., and Durbin, R. (2009). Fast and accurate short read alignment with Burrows-Wheeler transform. Bioinformatics *25*, 1754–1760.
86. Li, H., Handsaker, B., Wysoker, A., Fennell, T., Ruan, J., Homer, N., Marth, G., Abecasis, G., and Durbin, R.; 1000 Genome Project Data Processing Subgroup (2009). The Sequence Alignment/Map format and SAMtools. Bioinformatics *25*, 2078–2079.
87. Li, H. (2011). A statistical framework for SNP calling, mutation discovery, association mapping and population genetical parameter estimation from sequencing data. Bioinformatics *27*, 2987–2993.
88. Cingolani, P., Platts, A., Wang, L.L., Coon, M., Nguyen, T., Wang, L., Land, S.J., Lu, X., and Ruden, D.M. (2012). A program for annotating and predicting the effects of single nucleotide polymorphisms. SnpEff. Fly (Austin) *6*, 80–92.
89. Patro, R., Duggal, G., Love, M.I., Irizarry, R.A., and Kingsford, C. (2017). Salmon provides fast and bias-aware quantification of transcript expression. Nat. Methods *14*, 417–419.
90. Love, M.I., Huber, W., and Anders, S. (2014). Moderated estimation of fold change and dispersion for RNA-seq data with DESeq2. Genome Biol. *15*, 550–621.
91. Shiozaki, K., and Russell, P. (1997). Stress-activated protein kinase pathway in cell cycle control of fission yeast. In Methods in Enzymology, pp. 506–520.
92. Moreno, S., Klar, A., and Nurse, P. (1991). Molecular genetic analysis of fission yeast Schizosaccharomyces pombe. In Methods in Enzymology, pp. 795–823.
93. Erdeniz, N., Mortensen, U.H., and Rothstein, R. (1997). Cloning-Free PCR-Based Allele Replacement Methods. Genome Res. *7*, 1174–1183.
94. Bähler, J., Wu, J., Longtine, M.S., Shah, N.G., Mckenzie, A., III, Steever, A.B., Wach, A., Philippsen, P., and Pringle, J.R. (1998). Heterologous modules for efficient and versatile PCR-based gene targeting in Schizosaccharomyces pombe. Yeast *14*, 943–951.
95. McKenna, A., Hanna, M., Banks, E., Sivachenko, A., Cibulskis, K., Kernytsky, A., Garimella, K., Altshuler, D., Gabriel, S., Daly, M., and DePristo, M.A. (2010). The Genome Analysis Toolkit: A MapReduce framework for analyzing next-generation DNA sequencing data. Genome Res. *20*, 1297–1303.
96. Van der Auwera, G.A., Carneiro, M.O., Hartl, C., Poplin, R., del Angel, G., Levy-Moonshine, A., Jordan, T., Shakir, K., Roazen, D., Thibault, J., et al. (2013). From FastQ Data to High-Confidence Variant Calls: The Genome Analysis Toolkit Best Practices Pipeline. Curr. Protoc. Bioinforma. *43*, 483–492.
97. Oda, A.H., Tamura, M., Kaneko, K., Ohta, K., and Hatakeyama, T.S. (2022). Autotoxin-mediated latecomer killing in yeast communities. PLoS Biol. *20*, e3001844.
98. Lock, A., Rutherford, K., Harris, M.A., Hayles, J., Oliver, S.G., Bähler, J., and Wood, V. (2019). PomBase 2018: User-driven reimplementation of the fission yeast database provides rapid and intuitive access to diverse, interconnected information. Nucleic Acids Res. *47*, D821–D827.

STAR★METHODS

KEY RESOURCES TABLE

REAGENT or RESOURCE	SOURCE	IDENTIFIER
Antibodies		
Mouse anti-phospho-p70 S6K	Cell Signaling Technology	Cat#9206; RRID:AB_2285392
Rabbit anti-Spc1	Tatebe and Shiozaki[83]	N/A
Mouse anti-FLAG	Sigma-Aldrich	Cat#F3165; RRID:AB_259529
Mouse anti-DYKDDDDK tag	FUJIFILM Wako	Cat#012–22384; RRID:AB_10659717
Mouse anti-*myc*	Covance	Cat#MMS-150R-1000; RRID:AB_291325
Mouse anti-HA	Roche	Cat#11666606001; RRID:AB_514506
Rat anti-GFP	Nacalai Tesque	Cat#04404-84; RRID:AB_10013361
Goat anti-rabbit IgG (H + L) HRP-conjugated	Promega	Cat#W4011; RRID:AB_430833
Goat anti-mouse IgG (H + L) HRP-conjugated	Promega	Cat#W4021; RRID:AB_430834
Goat anti-Rat IgG (H + L) HRP-conjugated	Jackson ImmunoResearch Labs	Cat#112-035-003; RRID:AB_2338128
Chemicals, peptides, and recombinant proteins		
Rapamycin	LC Laboratories	Cat#R-5000
Protease inhibitor cocktail	Sigma-Aldrich	Cat#P8849
Lambda Protein Phosphatase	NEB	Cat#P0753S
SuperScript II reverse transcriptase	Thermo Fisher Scientific	Cat# 18064014
PowerUp SYBR Green Master mix	Thermo Fisher Scientific	Cat# A25741
Critical commercial assays		
RiboMinus Transcriptome Isolation Kit, yeast	Thermo Fisher Scientific	Cat# K155003
Deposited data		
DNA-seq data for WT_control	This study	DDBJ: DRR458346
DNA-seq data for Mutant_M2	This study	DDBJ: DRR503555
DNA-seq data for Mutant_M4	This study	DDBJ: DRR503556
DNA-seq data for Mutant_M5	This study	DDBJ: DRR503557
DNA-seq data for Mutant_M7	This study	DDBJ: DRR458347
DNA-seq data for Mutant_M10	This study	DDBJ: DRR503558
RNA-seq data for WT_replicate1	This study	DDBJ: DRR459935
RNA-seq data for WT_replicate2	This study	DDBJ: DRR459936
RNA-seq data for mks1Δ_replicate1	This study	DDBJ: DRR459937
RNA-seq data for mks1Δ_replicate2	This study	DDBJ: DRR459938
RNA-seq data for WT + rapamycin_replicate1	This study	DDBJ: DRR503559
RNA-seq data for WT + rapamycin_replicate2	This study	DDBJ: DRR503560
RNA-seq data for sck1Δ_replicate1	This study	DDBJ: DRR503561
RNA-seq data for sck1Δ_replicate2	This study	DDBJ: DRR503562
Experimental models: Organisms/strains		
S. pombe Haploid Deletion Mutant Set ver. 1.0	Bioneer	Cat#M-1030H
S. pombe Haploid Deletion Mutant Set ver 1.0 Upgrade Pkg	Bioneer	Cat#M-1030H-U
S. pombe Haploid Deletion Mutant Set ver 2.0 Upgrade Pkg	Bioneer	Cat#M-2030H-U

(*Continued on next page*)

Continued

REAGENT or RESOURCE	SOURCE	IDENTIFIER
S. pombe strain (*h-*)	Lab Stock	CA15458
Please see Table S5 for other *S. pombe* strains		
Oligonucleotides		
AAACCGAATCCTACGCAGCC	This study	mks1-F
CTGTGCGATGCGGAAAGTCT	This study	mks1-R
AAGCACCGAGGGTAACAAC	This study	hsp16-F
GGCCATTACTGAAGTTGGCCT	This study	hsp16-R
AAGTACCCCATTGAGCACGG	Lab stock	act1-F
CAGTCAACAAGCAAGGGTGC	Lab stock	act1-R
Recombinant DNA		
pFA6a-5FLAG-KanMX6	Noguchi et al.[84]	Addgene Plasmid #15983
pFA6a-5FLAG-hph	Lab stock	N/A
pFA6a-hph	Lab stock	N/A
pFA6a-mEGFP-KanMX6	Lab stock	N/A
pFA6a-13myc-hph	Lab stock	N/A
Software and algorithms		
GATK	Broad Institue	https://gatk.broadinstitute.org/hc/en-us
BWA	Li and Durbin[85]	https://bio-bwa.sourceforge.net/
Samtools	Li et al.[86]	https://samtools.sourceforge.net/
bcftools	Li[87]	https://samtools.github.io/bcftools/
SnpEff	Cingolani et al.[88]	https://pcingola.github.io/SnpEff/
Salmon (version 1.1.0)	Patro wt al.[89]	https://combine-lab.github.io/salmon/
DESeq2	Love et al.[90]	https://bioconductor.org/packages/release/bioc/html/DESeq2.html

RESOURCE AVAILABILITY

Lead contact

Further information and requests for resources and reagents should be directed to and will be fulfilled by the lead contact, Yuichi Morozumi (y-morozumi@bs.naist.jp).

Materials availability

S. pombe strains generated in this study are available upon request to the lead contact.

Data and code availability

- The whole-genome sequence and RNA sequence data have been deposited at the DDBJ Sequence Read Archive (DRA) and are publicly available as of the date of publication. Accession numbers are listed in the key resources table.
- This paper does not report original code.
- Any additional information required to reanalyze the data reported in this paper is available from the lead contact upon request.

EXPERIMENTAL MODEL AND STUDY PARTICIPANT DETAILS

Fission yeast strains and general methods

S. pombe strains used in this study are listed in Table S5. Cells were grown in YES medium containing 3% glucose at 30°C unless indicated otherwise.[91,92] For the strain constructions, the PCR-based method was applied to introduce amino acid substitutions, truncations, and the epitope tag sequences to chromosomal genes.[93,94] The DNA fragments approximately 500 bp upstream and downstream of the target regions were amplified using *S. pombe* genomic DNA as the template. The reverse primer for the upstream fragment and forward primer for the downstream fragment contain the homologous sequence to the upstream (5′-TTAATTAACCCGGGGATCCG-3′) and downstream (5′-CA GATCCACTAGTGGCCTAT-3′) of a pFA6a plasmid cassette, respectively. After the purification of DNA fragments, PCR was again performed

using the amplified fragments and a pFA6a plasmid derivative[84] listed in the key resources table that contains the desired epitope tag and selection marker as templates to amplify two fragments that harbor an overlapping region within the selection marker. The amplified DNA fragments were then co-transformed into *S. pombe* cells to replace the endogenous region through homologous recombination. Transformants were selected under a selection plate and checked by PCR. Each introduced amino acid substitution and truncation was confirmed by genomic PCR followed by Sanger DNA sequencing. The strains that carry the same selection marker at two different loci were constructed by crossing.

METHOD DETAILS

S. pombe growth assay

Fission yeast cells were grown in YES liquid medium, and the cultures were adjusted to the cell concentration equivalent to an optical density at 600 nm (OD_{600}) of 1.0. Serial dilutions of the adjusted cultures were spotted onto agar solid media. Images were captured by the LAS-4000 system (Fujifilm, Japan). For the growth curve assay, cells were grown in YES liquid media at 30°C. Overnight cultures were adjusted to initial OD_{600} = 0.1 in fresh media, and cell density was measured at indicated time intervals. For heat treatment at 39°C, the overnight cultures were resuspended in pre-warmed fresh media.

Cell viability assay

Cells were suspended in 1× PBS buffer, pH 7.4 (40 mM K_2HPO_4, 10 mM KH_2PO_4, 0.15 M NaCl). The cell suspension was then mixed with methylene blue (0.1 mg/mL stock solution) in a 1:1 ratio and incubated for 2 min at room temperature. Cell viability was examined under the microscope, and stained cells were counted as dead cells. At least 200 cells were counted for each experiment.

Immunoblotting

Cells grown in YES medium were mixed with trichloroacetic acid at a final concentration of 10% and harvested. Collected cell pellets were then suspended in 10% trichloroacetic acid and vortexed vigorously with 0.5-mm-diameter zirconia beads for 5 min at 4°C. After breakage, cell suspensions were centrifuged at 800 × g for 10 min, and the supernatant was discarded. The remaining pellets were suspended in the SDS sample buffer containing 0.5 M Tris-HCl (pH 8.0) and boiled for 5 min, followed by centrifugation at 17,700 × g for 15 min. The recovered supernatant was separated by SDS-PAGE, transferred to nitrocellulose membrane, and probed with primary antibodies listed as follows; anti-phospho-p70 S6K (1:5000; Cell Signaling Technology) for phosoho-Psk1 (Thr-415) detection, anti-Spc1 (1:10000),[83] anti-FLAG (1:5000; Sigma-Aldrich) and anti-DYKDDDDK (1:5000; FUJIFILM Wako) for the FLAG-tagged protein detection, anti-*myc* (1:5000; Covance), anti-HA (1:2000; Roche) and anti-GFP (1:2500; Nacalai Tesque). Anti-rabbit IgG (H + L) HRP-conjugated (1:10000; Promega), anti-mouse IgG (H + L) HRP-conjugated (1:10000; Promega), and anti-rat IgG (H + L) HRP-conjugated (1:10000; Jackson ImmunoResearch) were used as secondary antibodies.

S. pombe deletion library screen

The Bioneer *S. pombe* haploid deletion library used in this study contains 3,400 haploid deletion mutants with 95.8% genome coverage. All mutants are auxotrophs for adenine (*ade6-M210*), uracil (*ura4-D18*), and leucine (*leu1-32*) harboring KanMX4 as a selection marker. The deletion mutants in the library were spotted onto solid YES medium in the presence and absence of 100 ng/mL rapamycin and incubated at 30°C and 39°C. An initial screening isolated 41 candidate mutant strains whose growth at high temperatures was further tested by spotting serial dilutions of their cultures on YES agar plates in the presence and absence of 100 ng/mL rapamycin. During this step, 9 mutant strains were selected, and gene deletion as well as co-segregation of the selection marker and high-temperature growth phenotype were examined by genomic PCR and tetrad analysis, respectively. Finally, the 5 genes shown in Figure 3A were identified as suppressors of cell growth at high temperatures. Prototrophic mutant strains were obtained by crossing with a wild-type strain and were further used in this study.

Immunoprecipitation assay

Yeast cells were disrupted in lysis buffer (20 mM HEPES-NaOH [pH 7.5], 150 mM sodium glutamate, 10% glycerol, 0.25% Tween 20, 10 mM sodium fluoride, 10 mM *p*-nitrophenylphosphate, 10 mM sodium pyrophosphate, 10 mM β-glycerophosphate and 0.1 mM sodium orthovanadate), containing 1 mM PMSF and protease inhibitor cocktail (Sigma-Aldrich) with glass beads using Multi-beads Shocker (Yasui Kikai). The cell lysate was recovered by centrifugation for 15 min at 17,700 × g and the total protein concentrations of cell lysates were determined by Bradford assay. For interaction between FLAG- and myc-tagged proteins, the recovered cell lysates were incubated with anti-FLAG M2-affinity gel (Sigma-Aldrich) for 2 h at 4°C, followed by extensive washes with lysis buffer. Resultant samples were subjected to immunoblotting.

For interaction between FLAG-tagged Mks1 and GFP-tagged Rad24, and between the myc-tagged Mip1 and FLAG-tagged Mks1, cell lysates were incubated with anti-FLAG antibodies (FUJIFILM Wako) and anti-myc antibodies, respectively, for 1 h at 4°C, followed by incubation with Dynabeads Protein G (Invitrogen) for 2 h at 4°C.

Phosphatase treatment

10-20 μg of total protein prepared using trichloroacetic acid was treated with Lambda Protein Phosphatase (NEB) in the presence of a phosphatase inhibitor mixture (2 mM sodium orthovanadate, 10 mM EDTA, 10 mM sodium fluoride, 4 mM *p*-nitrophenylphosphate and 10 mM

β-glycerophosphate) at 30°C for 2 h according to the manufacturer's protocol. After incubation at 65°C for 1 h, the resultant samples were subjected to immunoblotting.

Isolation of spontaneous mutants that can grow at high temperatures

1×10^7 of wild-type cells grown in YES liquid medium to exponential phase at 30°C were spread on YES agar medium and incubated at 39°C. Ten viable colonies were then isolated, and their growth at 39°C was confirmed by spotting serial dilutions of their cultures on YES agar plates. Five spontaneous mutants that exhibited significant cell proliferation at 39°C were selected, and their genome was analyzed by whole-genome sequencing to determine mutations responsible for the high-temperature growth phenotype.

Whole-genome sequencing and data analysis

Cells were grown in YES liquid medium to exponential phase at 30°C and harvested by centrifugation. Genomic DNA was extracted and purified using NucleoBond AXG and Buffer Set III (MACHEREY-NAGEL) according to the manufacturer's protocol. Whole-genome sequencing was performed by BGI JAPAN using a DNBseq platform, and the sequencing reads were mapped to the *S. pombe* reference genome using BWA[85] and samtools,[86] followed by variant calling using GATK HaplotypeCaller.[95,96] The mutations specifically found in the mutant strains were extracted and annotated using bcftools[87] and SnpEff,[88] respectively.

RNA extraction, RT-qPCR and RNA-seq

Cells were grown to exponential phase at 30°C and shifted to 39°C for heat treatment experiment. Cells were harvested through filtration onto 0.45 μm mixed cellulose ester membrane (Advantec) and flash-frozen using liquid nitrogen. The cell pellets were resuspended in a pre-heated (65°C) solution composed of 25 μL of 10% SDS and 300 μL of acid phenol: chloroform, and acid-washed glass beads and bead buffer (75 mM NH_4OAc and 10 mM EDTA, pH8) were then added. The samples were vigorously mixed using a vortex mixer for 1 min, and subsequently incubated at 65°C for 1 min. After repeating this process 3 times, the aqueous phase was recovered through centrifugation at 16000 × *g* for 15 min and transferred into 250 μL of pre-warmed bead buffer. The samples were further subjected to centrifugation at 16,000 × *g*, 4°C for 15 min and the supernatant was mixed with prechilled bead buffers containing isopropanol. After centrifuging at 22,000 × *g*, 4°C for 30 min, the pellets were washed with RNase-free 70% ethanol, dried and dissolved in 30 μL of DEPC water.

For qPCR, the SuperScript II reverse transcriptase (Thermo Fisher Scientific) was used to synthesize cDNA according to the manufacturer's protocols. qPCR was carried out using PowerUp SYBR Green Master mix (Thermo Fisher Scientific) with the primers listed in the key resources table. The results were normalized against the housekeeping gene *act1*$^+$.

For RNA-seq, cDNA libraries of two biological replicates for wild-type cells with or without rapamycin treatment, as well as the *sck1*Δ and *mks1*Δ strains were prepared following the previous paper,[97] except the step of rRNA removal that was performed using RiboMinus Transcriptome Isolation Kit, yeast (Thermo Fisher Scientific). Paired end sequencing was performed using Illumina HiSeq (300 cycles), and gene expression level was calculated using Salmon (version 1.1.0)[96] and the R package "DESeq2".[90] Genes expressed with adjusted p values <0.1 were considered as differentially expressed genes. The reference genome sequence and gene annotation information of S. pombe were obtained from the PomBase database (http://www.pombase.org).[98] GO categories of the target genes were determined in PomBase using GO Term Finder (https://go.princeton.edu/cgi-bin/GOTermFinder).

QUANTIFICATION AND STATISTICAL ANALYSIS

Statistical analyses were performed using the R package DESeq2 or Microsoft Excel software. Details of particular statistical analyses and statistical significance are included in the corresponding figure legends.